Synthesis of Activated Carbon from *Prosopis Juliflora* Wood for the Removal of Phosphate from Municipal Wastewater

Yohannes Garuma Ede

A Thesis Submitted to the Department of Applied Chemistry

School of Applied Natural Science

Presented in Partial Fulfillment of the Requirement for the Degree of Master's in Applied Chemistry (Industrial Chemistry)

Office of Graduate Studies

Adama Science and Technology University

January, 2024
Adama, Ethiopia

Synthesis of Activated Carbon from *Prosopis Juliflora* Wood for the Removal of Phosphate from Municipal Wastewater

Yohannes Garuma Ede

Advisor: Fedlu Kedir (Ph.D.)

A Thesis Submitted tothe Department of Applied Chemistry

School of Applied Natural Science

Presented in Partial Fulfillment of the Requirement for the Degree of Master's in Applied Chemistry (Industrial Chemistry)

Office of Graduate Studies

Adama Science and Technology University

January, 2024

Adama, Ethiopia

Synthesis of Activated Carbon from *Prosopis Juliflora* Wood for the Removal of Phosphate from Municipal Wastewater

Yohannes Garuma Ede

Advisor: Fedlu Kedir (Ph.D.)

A Thesis Submitted tothe Department of Applied Chemistry

School of Applied Natural Science

Presented in Partial Fulfillment of the Requirement for the Degree of Master's in Applied Chemistry (Industrial Chemistry)

Office of Graduate Studies

Adama Science and Technology University

January, 2024

Adama, Ethiopia

APPROVAL SHEET

I, the advisor of the thesis entitled "**Synthesis of Activated Carbon form *Prosopis Juliflora* Wood for the Removal of Phosphate from Municipal Wastewater**" and developed by Yohannes Garuma Ede; hereby certify that the recommendation and suggestions made by the board of examiners are appropriately incorporated into the final version of the thesis.

Fedlu Kedir (PhD)	_____	_____
Major Advisor	Signature	Date

We, the undersigned, members of the Board of Examiners of the thesis by Yohannes Garuma Ede, have read and evaluated the thesis entitled "**Synthesis of Activated Carbon form *Prosopis Juliflora* Wood for the Removal of Phosphate from Municipal Wastewater**" and examined the candidate during open defense. This is, therefore, to certify that the thesis is accepted for partial fulfillment of the requirement of the degree of Master of Science in Applied Chemistry (Specialization in Industrial Chemistry).

_____	_____	_____
Chairperson	Signature	Date
_____	_____	_____
Internal Examiner	Signature	Date
_____	_____	_____
External Examiner	Signature	Date

Final approval and acceptance of the thesis is contingent upon submission of its final copy to the Office of Postgraduate Studies (OPGS) through the Department Graduate Council (DGC) and School Graduate Committee (SGC)

_____	_____	_____
Department Head	Signature	Date
_____	_____	_____
School Dean	Signature	Date
_____	_____	_____
Office of Postgraduate Studies, Dean	Signature	Date

DECLARATION

I hereby declare that this Master Thesis entitled "**Synthesis of Activated Carbon form *Prosopis Juliflora* Wood for the Removal of Phosphate from Municipal Wastewater**" is my original work. That is, it has not been submitted for the award of any academic degree, diploma or certificate in any other university. All sources of materials that are used for this thesis have been duly acknowledged through citation.

_____	_____	_____
Name of the Student	Signature	Date

RECOMMENDATION

I, the advisor of this thesis, hereby certify that I have read the revised version of the thesis entitled "**Synthesis of Activated Carbon form *Prosopis Juliflora* Wood for the Removal of Phosphate from Municipal Wastewater**" prepared under my guidance by Yohannes Garuma Ede submitted in partial fulfillment of the requirements for the degree of Masters of Science in Applied Chemistry (Industrial Chemistry). Therefore, I recommend the submission of revised version of the thesis to the department following the applicable procedures

Fedlu Kedir (PhD) _____ _____

Major Advisor Signature Date

ACKNOWLEDGMENT

Above of all, I would like to express my deepest gratitude to Almighty God for all kinds of aptitude, wisdom, knowledge, strength, and patience to accomplish my thesis work.

I'm deeply thankful to my advisor Dr. Fedlu Kedir, for his deep interest, patient advice, professional guidance, constructive comments, and close follow-up spending his time, encouragement, and supervision throughout this study.

I want to thank Adama Science and Technology University (ASTU), School of Applied Natural Science, Department of Applied Chemistry, for giving me the chance to upgrade myself in this M.Sc. program and for supporting me with the available resources for doing my work.

I greatly acknowledge Ato Abera Degafa from Metahara Sugar Factory, Research department Coordinator for his sport in laboratory facility; Ato Tsegaye Markos from Jimma University (JU), Department of Material Science and Engineering for XRD characterization, Ato Alebel Abebaw from Bahir Dar University (BDU), Department of Chemical Engineering for FTIR characterization, Ato Leta Guta from Adama Science and Technology University (ASTU), Department of Applied Biology for SEM characterization, Ato Aseged Bekele from Addis Ababa Science and Technology University (AASTU), Department of Chemical Engineering for his assistance in BET characterization.

Finally, I would like to give a huge thank to my wife (Hayat Hassen), my children (Fenet Yohannes, Bilise Yohannes and Soninaf Yohannes), Rukiya Hassen, friends and colleagues who have supported me in completing this thesis.

TABLE OF CONTENTS

LIST OF TABLES

LIST OF FIGURS

LIST OF ABBREVATIONS

AC	Activated Carbon
APHA	American Public Health Association
ASTU	Adama Science and Technology University
BET	Brunauer-Emmet- Teller
EPA	Environment Protection Agency
EU	European Union
ESIG	Ethiopian Sugar Industry Group
FTIR	Fourier transform-infrared spectroscopy
HABs	Harmful algal blooms
IUPAC	International Union of Pure Applied chemistry
KPJAC	Potassium hydroxide treated *Prosopis Juliflora* Activated Carbon
KSM	Kessem Sugar Factory
MSF	Metahara Sugar Factory
P	Phosphate ions
PJAC	*Prosopis Juliflora* Activated carbon
PJ	*Prosopis Juliflora*
PJBM	*Prosopis Juliflo*ra Biomass
SEM	Scanning Electron Microscope
SIG	Sugar Industry Group
USEPA	United States Environmental Protection Agency
UV-Vis	Ultraviolet-Visible Spectroscopy
WHO	World Health Organization
XRD	X- ray diffraction

ABSTRACT

Surface water contamination with phosphate ions is resulting in eutrophication. The adsorption of phosphate from wastewater by activated carbon prepared from highly available carbonaceous natural plant biomass is one of the successful methods. Prosopis Juliflora is one of the massive invaded weeds in the Kessem Sugar Factory state that highly reduces productivity. Preparing activated carbon from PJ biomass by impregnation using chemical reagents is one of the mechanisms to control the distribution and limit the effect. Samples from the infested sugarcane field at KSM were collected, chopped, and ground. It was then impregnated for 24 hours at a 1:1 ratio with potassium hydroxide in water, oven-dried for 24 hours, and pyrolyzed for two hours at 400, 500, and 600℃ at a heat rate of 10℃/m to produce PJAC, which was then labeled (KPJAC400, KPJAC500, and KPJAC600). X-ray diffraction, Fourier transform infrared spectroscopy, Scanning Electron Microscopy, and Brunauer-Emmett-Teller were used to characterize the sensitized activated carbon. The prepared activated carbon's surface area is 547.127 m2/g. Using batch adsorption techniques, the KPJAC500 adsorbent's performance in phosphate removal was evaluated, and the effects of several factors such as temperature, adsorbent dose, initial phosphate concentration, contact time, and solution pH were examined. According to the results, the adsorption effectiveness is optimal at pH 4, an adsorbent dosage of 4 g/L, a 180-minute contact period, and a 25 mg/L starting phosphate concentration at 30℃. Applying optimized parameters, the kinetic and adsorption isotherm models were studied. In addition, the effect of interfering ions and the efficiency of the regeneration of the adsorbent were determined. The maximum phosphate removal efficiency of the adsorbent in optimal circumstances from aqueous solutions and wastewater was 84.6% and 52.3%, respectively. The maximum adsorption capacity of activated carbon in the optimal situation was obtained to be 10.6 mg/g. From the tested adsorption isothermal model, the Langmuir model was investigated to be the best fit, and from the kinetics of the adsorption process models, pseudo-second-order kinetics fit well. The interfering ions evaluation results show that the phosphate adsorption efficiency was affected by ions. In the present study, the elution results showed that reusing an adsorbent to remove phosphate from an aqueous solution was promising.

Keywords: *Adsorption, Activated Carbon, Phosphate, Pollutant, Prosopis Juliflora*

1. INTRODUCTION

1.1. Background

Water is the most essential natural resource for all living species, and there would be no life without it. Surface water is applicable for many benefits such as: consumption, irrigation, transportation, industries, and recreational activities. However, water is a limited resource, and only a small fraction of the total amounts of water is usable for different purposes. 72% of the Earth is occupied in water, but saline water in the oceans takes up over 96 percent. Thus, the remaining (about 3%) is fresh water, of which approximately 99.7% is bagged in icecaps and glaciers or stored in groundwater aquifers. Surface water only amounts to about 0.3% of all freshwater worldwide. This limited resource is becoming dramatically polluted due to anthropogenic activities (Constantin *et al.,* 2021).

Recently, rapid expansion of urban and population has interested higher water demands, which tend to generate excess volume of wastewater that has high contribution to degradation of surface water quality. Surface water has become more susceptible to contamination by sewage, industrial pollution and agricultural runoff as a result of a significant increase of urban population (S. Kumar *et al.,* 2021). In developing countries, surface water pollution low level due to weak economic growth. Currently, lakes of Ethiopia specifically Lake Tana, and Hawasa have been exposed for pollution due to the following factors: excessive water withdrawal, population increase, rising living standards, intensive farming practices, and industrial developments. These resulted in significant changes in physiochemical, biological structures and dynamics of the lakes and other fresh waters, often showing a significant shift from clear water to contaminate. As a consequence, water pollution and coverage of water eutrophication are currently a major's environmental challenge in Lake Tana and Hawasa. (Tibebe *et al.,* 2019: Menberu *et al.,* 2021).

In aquatic environment phosphate naturally occurs in small amounts and is vital for maintaining the development and metabolism of aquatic flora and fauna. However, the most actives form of phosphate (orthophosphate) can be proven aquatic harmful in excess amounts. Phosphate pollution has become one of the significant environmental concerns due to dramatic increases of discharge, it can cause for algae bloom and eutrophication when it is

present in on in the surface of water (Recepoglu *et al.,* 2022). To control the effect of it, the World Health Organization (WHO) recommended phosphate concentration less than 5 mg/L in natural water (Gamshadzehi *et al.,* 2019). In European Union (EU) countries recommended phosphate discharge to sensitive water bodies such as lakes and rivers is set less than 0.01 and 0.07 mg/L, respectively (Kim *et al.,* 2019). However, according to Environmental Protection Authority (EPA) in 2003 guideline total phosphorus standard limitation discharge rate is 5 mg/L (EPA, 2003). For that reason, recovery of phosphate from wastewater before its discharging into the environment is critical in order to meet the standard limit and reducing its negative effects.

Concerning wastewater treatment technology, various techniques have been studied to recover phosphate. They fall into three main categories: biological, chemical, and physical. Physical methods such as reverse osmosis and electro dialysis are too expensive, whereas others are ineffective, reaching only 10% removal efficiency. Enhanced biological treatment method can achieve best removal of total phosphorus, but operational difficulties make it unstable. Chemical techniques are the most effective and well-studied methods, including phosphate precipitation with different salts such as calcium and aluminum (Siyal *et al.*, 2020). However, this method has not been practical due to high salts consumption increases the costs, and the amount of sludge generated. Therefore, to recover phosphate from wastewater requires other effective and ecofriendly techniques.

Adsorption is one of the most important approaches to pollutant removal from wastewater. It is the process of accumulating chemical substances onto a surface or interface. The adsorbing phase is defined as the adsorbent, and the material being adsorbed is the adsorbate. The adsorbent is required to have an extremely large surface area on which the adhesion of contaminants can occur. It can occur between two phases, such as the gas-liquid, gas-solid, liquid-liquid, or liquid-solid interface. In the field of water treatment, adsorption has been proven to be an efficient removal process for numerous types of pollutants, where ions or molecules are removed from liquids by adsorption onto solid surfaces. In addition It is easy to operate as it requires a relatively simple design, offers the possibility of adsorbent regeneration, and results in a low amount of waste (Almanassra *et al.,* 2020).

Various adsorbents have been studied for phosphate remediation from aqueous solutions, such as zeolite (Rallapalli & Ha, 2020), polymeric adsorbents (Ritt *et al.*, 2019) , porous silica, activated carbon and clay minerals (Bacelo *et al.*, 2020). From these adsorbents, activated carbon has been widely used for phosphate recovery due to its porous structure, stability, and high surface area. However, several activated carbons often have hydrophobic or very weak charge groups on the surface, thus establishing a poor phosphate adsorption capacity. In this regard, activated carbon was impregnated with alkali metal oxide, alkaline hydroxide, and metal ions to enhance their phosphate adsorption (Bacelo *et al.*, 2020; Mojoudi *et al.*, 2019).

Investigation has been increasing seriously to find an alternative and develop low-cost adsorbent materials from easily available and less expensive agricultural byproducts (Jack *et al.*, 2019). Adsorbents prepared from agricultural byproducts have high porosity and are insoluble in water. The adsorbing quality of the prepared activated carbon depends on the activating agent, impregnation ratio, activating time, carbonized temperature, and the presence of inorganic impurities. When such materials are prepared as sorbents for their proposed task, the functional groups on the adsorbent surface are responsible for pollutant sorption (Kumar *et al.*, 2010).

Prosopis Juliflora (PJ) is declared a noxious weed in Africa and Asian countries, including Ethiopia, because of its economic and environmental impact. It displaces native flora and fauna, depleting the water resource and threatening crop production by affecting soil nutrients (Shiferaw *et al*., 2021). In order to minimize the adverse impact and maximize benefit, control and management of PJ distribution are crucial. Therefore, the synthesis of activated carbon using PJ biomass is one of the significant mechanisms to control the distribution of the weed (Sato, 2013).

This study aimed to prepare activated carbon derived from the woods of PJ using potassium hydroxide as impregnating (socking) and evaluate the phosphate removal efficiency of the adsorbent from an aqueous solution. The effectiveness of the developed adsorbent was tested under adsorption parameters such as solution pH, adsorbent dose, phosphate initial

concentration, contact time, and temperature. Also, the adsorption efficiency of the adsorbent for real wastewater was evaluated under optimal adsorption parameters.

1.2. Statement of the Problem

Phosphate is one of the critical pollutants in the water ecosystem, which causes the growth of harmful algae that leads to eutrophication (Lee *et al.*, 2017). The harmful algal blooms (HABs) cause an odor nuisance to the atmosphere and gastrointestinal and respiratory issues in humans due to cyanotoxins (Lalley *et al*., 2016). In addition to determinant effects on human and aquatic life, growth (HABs) has greater impacts on the national economy as it adversely affects tourism, drinking water availability, and the fisheries sector.

Adsorption is preferred due to its economic advantage and practicability for the recovery of pollutants from wastewater (Ghorbani *et al.,* 2020). Commercial activated carbon is widely utilized as an adsorbent for the removal of pollutants from aqueous solutions; however, it is extremely expensive because of the use of non-renewable and relatively expensive starting materials that are prone to exhaustion. In particular, agricultural-based biomass-activated carbons have high attention due to cost effectiveness, renewability, and affordability.

Prosopis Juliflora species is a major problem in arid and semi-arid areas of the sugar industry in Ethiopia. It is a noxious weed heavily infesting most agriculture as well as potential rangeland (Tegene *et al.*, 2019). Recently, at Kessem sugar factory (KSF), a high infestation of PJ weed was observed on lands such as along irrigate canals, drainage land, around residences, harvest roads, and the main road side. The presence of this invasive alien species as any weed in a sugar cane field highly suppresses the crop through its competition for light, air, and nutrients, resulting in reduced cane yields per hectare and increased production costs. Therefore, this work can solves the problem using JP Wood biomass as raw material for preparation of ACs for adsorption phosphate.

1.3. Objective

1.3.1. General Objective of the Study

The objective of this study was to synthesize activated carbon from *Prosopis Juliflora* wood for the removal of phosphate from municipal wastewater.

1.4. Specific Objective

- To prepare AC using activating agent and pyrolysis methods at 400, 500, and 600℃.
- To characterize the as-synthesized absorbents by FTIR, BET, XRD, and SEM.
- To optimize adsorption parameters (pH, contact time, adsorbent dose, initial phosphate concentration, and temperature) for the removal of phosphate from an aqueous solution.
- To compare the adsorption efficiency of impregnated AC and pristine AC.
- To check adsorption kinetic models.

1.5. Significance of the Study

The adsorption technique investigated to remove phosphate that poses a series of health and environmental hazards in this study appears promising as an inexpensive, efficient, effective, economically feasible, obtainable, and environmentally friendly technique.

- The prepared activated carbon PJAC can be used to remove phosphate from wastewater from different domestic effluents before being discharged into the environment.
- The research will contribute to providing insight on how to develop a simple, cost-effective, environmentally friendly, and easily available activated carbon adsorbent that can be used to substitute imported activate carbon or other expensive and environmentally unfriendly materials.
- The conversion of *Prosopis Juliflora* biomass into valuable PJAC helps to reduce groundwater depletion because of the plant, increase the availability of productive land, and increase the productivity of crops and livestock.
- Using the described agricultural waste biomass as an adsorbent could be a good solution to control the expansion of the species and create additional job opportunities.
- This study might be important for governmental organizations engaged in wastewater treatment and small-scale business stakeholders.

2. LITERATURE REVIE

Understanding some of the related literature from previous studies is important for any research in order to discover prime techniques that could assist as a guiding framework for research progress. The literature review of this study is organized and discussed as follows:

2.1. Water Pollution

Water is one of the essential natural resources needed to sustain life on earth and has a significant challenge in modern agriculture, ecosystems, and health. Contaminated water is a major ecological issue that influences both humans and the environment, resulting in substantial economic and social crises. Water quality has been polluted intensely as a result of human activity, population growth, fast industrialization, radical urbanization, and unmanaged use of natural water resources, among other factors (Chowdhary *et al.*, 2020).Contaminants in wastewater, generated from a variety of sources in different amounts, reach the environment either directly or indirectly, causing harm.

Water contamination is caused by various organic and inorganic pollutants, which are basically generated from domestic, industrial, and agricultural activities (Breulmann *et al.*, 2018). Disposal of organic and inorganic compounds generated from different industries, such as cosmetics, leather, plastic, paper, and pharmaceutical industries, has received high attention globally in recent years because those effluents contain various types of toxic and carcinogenic contaminants Heavy metals, chemical fertilizers, and nutrients, including phosphate, on the other hand, rise in various amounts as environmental hazards and inorganic contaminants (Sahoo *et al.*, 2019).

Phosphate pollution has become one of the most significant environmental issues due to the intensive increase in discharges from urbanization, agricultural runoff, and industrial activities. Even though phosphate is a primary nutrient for plant growth and germination, it can accelerate algae blooms and cause eutrophication when the amounts of phosphate exceed 0.25 mg L^{-1} in surface water (Recepoglu *et al.*, 2022). Water eutrophication resulting from algae overgrowth can threaten human health, destroy the self-purification capacity of water, cause detrimental effects to aquatic systems, and deteriorate water quality (Buates & Imai, 2020; Yin *et al.*, 2018). In Ethiopia, where economic development is so young, most surface

water is relatively unspoiled. However, the first sign of eutrophication was observed in Hawassa and Tana Lake (Fetahi, 2019; Moges *et al.*, 2017). Phosphate pollution in Ethiopia arises from different sources, such as urban and domestic effluent, agricultural runoff, and industrial activity (Genanaw *et al.*, 2021). Therefore, effective control of phosphate contamination has been attracting a great deal of attention currently. Moreover, the sustainable management of phosphate plays an important role in terms of environmental and economic perspectives.

To control eutrophication, according to the WHO in 2006, the recommended standard for discharging industrial wastewater is a phosphate concentration of 2 mg/L. The permitted limit of phosphate concentration is 0.05 mg/L in streams discharged into lakes or reservoirs, 0.25 mg/L in a lake or reservoir, and 0.1 mg/L in river waters (WHO, 2006). The United States Environmental Protection Agency (USEPA) has set the limited value for phosphorus discharge at a range of 0.05–0.1 mg/L in a stream at a point source disposed to a lake or reservoir (Loganathan *et al.*, 2014). In addition, according to European Union (EU) countries, phosphate discharge to sensitive water bodies such as lakes and rivers is set to be less than 0.01 and 0.07 mg/L, respectively (Berkessa *et al.*, 2019). However, according to the Ethiopian Environmental Protection Authority's (EPA) 2003 guideline, the total phosphorus standard limitation discharge rate is 5 mg/L (EPA, 2003). Therefore, phosphate above the permitted limit value has an impact on the ecosystem. Table 2.1 illustrates the phosphate concentration reported in the literature for aqueous solutions from different sources.

Table 2.1: Comparison of phosphate level in wastewater from different sources

Wastewater type	PO_4^{3-} mg/L	Reference
Urine (unmixed)	470 - 1070	(Randall & Naidoo, 2018)
Untreated domestic waste	17.2 – 216.17	(Lewoyehu *et al.*, 2022)
Secondary treated waste	5-10	(Egle *et al.*, 2015)
Slaughters house wastewater	28.6 – 67.33	(Mulu *et al.*, 2013)
Beverage industries wastewater	0.185 – 69.7	(Abrha & Chen, 2017)
Distillery spent wash wastewater	21.2	(Fito, Tefera, *et al.*, 2019)
Dairy industry	350 - 450	(S. Wang *et al.*, 2009)

2.1.1. Phosphate

Phosphorus is a primary nutrient and essential for the growth of plants and other biological organisms. Phosphorus occurs in waters and wastewaters as phosphates in three forms: orthophosphates, condensed phosphates, and organic phosphates (APHA, 2012). Orthophosphate can be found under different species, H_3PO_4, $H_2PO_4^-$, HPO_4^{2-}, and PO_4^{3-}, depending on the pH and in accordance with the dissociation constants: $pK_1 = 2.21$, $pK_2 = 7.21$, and $pK_3 = 12.67$ (Bacelo *et al.,* 2020) and presented in Equation 1. The available form of phosphorus in wastewater is determined by soluble reactive phosphorus (SRP) and the ratio of orthophosphate to SRP (Maruo *et al.,* 2016; Comber *et al.,* 2015). Natural and biological oxidation processes usually transform more complex forms of phosphorus into orthophosphates, which are the most common form and the only type that can be assimilated by most plants (Nejad *et al.,* 2013).

$$H_3PO_4 \xrightarrow{pK_1 = 2.2} H_2PO_4^- \xrightarrow{pK_2 = 7.2} HPO_4^{2-} \xrightarrow{pK_3 = 12.6} PO_4^{3-} \quad \text{..... Eq. 1}$$

2.1.2. Source of Phosphate

In nature, phosphate is usually the influencing nutrient in water bodies like lakes and rivers. In order to control the eutrophication process, the inputs of phosphate to water bodies must be managed. This can be accomplished by sorting the sources of phosphate and potential extenuation methods for redaction. Phosphate enters the aquatic environment from a variety of sources, both point and non-point. The natural sources (non-points sources) of aqueous phosphate water bodies include weathering rock and decomposition organic matter, erosion, storm water runoff, sedimentation, and atmospheric deposition (R. Li *et al.,* 2017), but the major source of aqueous phosphate is anthropogenic activity that includes municipal and agricultural runoff, discharge from wastewater treatment facilities, and industrial discharge (Mohan *et al.,* 2014).

2.1.3. Adverse Effect Phosphate

Eutrophication is considered by the large amounts of production of algae and plants in water and an ecosystem as a result of an increment in phosphate discharge above the permitted limit (Yuan *et al.,* 2019). Naturally, eutrophication happens in water bodies over a long period of time as they age and are filled with sediments. However, the dramatic growth of

agricultural and industrial activities and increasing economic growth, due to exponential population growth, have sped up the rate and extent of eutrophication due to the excessive presence of phosphate in aquatic systems (Carpenter, 1981).

The disposal of these contaminants in excessive amounts causes eutrophication of water, which establishes, at first, large-grown algae, aquatic plants, and cyanobacteria. That water becomes anoxic and disturbs the natural habitat of fish. The process is then followed by the decomposition of flora with the release of carbon dioxide and decreasing pH, which influence the growth and development of the respective fauna. Eutrophication is a phenomenon that affects the ecosystem as well as economic, social, and recreational activities over time (Lamberti *et al.,* 2010).

Various characteristics of the water ecosystem can be negatively influenced by eutrophication, resulting in intensive algae growth (Huisman & Hulot, 2005; Fan *et al.,* 2020). Harmful algae blooms (HABs) are one of the growing threats to water ecosystems. They may cause destructive impacts on both flora and fauna in ecosystems through activities such as poisoning by toxins (Ramanan *et al.,* 2016). Cyanobacteria, which blooms as the most harmful algae, can cause much pain or damage to the environment, the production of hepatotoxins and neurotoxins (Lee *et al.,* 2017), and human death (H. Li & Pan, 2015). In addition, HABs indirectly affect marine animals because they pose threats to the health and reproduction of invertebrates. The truism value of eutrophic waters is reduced as a result of the unpleasant odor and view. Overplant growth can hinder marine transport. If the water is demanded for potable use, the costs of treatment are challenged by others (Huang *et al.,* 2014). Many algae release neurotoxins, which have detrimental effects on fish, mussels, and other livestock. Therefore, the fishery industry is damaged due to job insecurity (Ramanan *et al.,* 2016).

2.2. Phosphate Removal Method

Phosphate remediation from wastewater to control the emergence of eutrophication in natural water is mostly achieved by physical, chemical, and biological processes (You *et al*., 2016). The phosphate remediation capacity of physical treatment methods is very low, and those efficient ones, such as electro-dialysis and reverse osmosis, are comparatively expensive.

Chemical precipitation is a practical method to remove phosphate from wastewater. However, chemical treatment methods are not effective due to the high operational cost of chemicals and the large chemical sludge volumes (up to 40%) that are difficult to dispose of, and the neutralization of effluent has limitations (Vasudevan & Rangaiah, 2011). Table 2.2 shows the advantages of the main conventional technology used for the removal of phosphate from water and wastewater effluents. Biological methods require carbon resources and a long period of microbial culturing. This method of phosphate removal efficiency usually does not exceed 30%. The effluent quality leftovers are high above discharge standard limits (You *et al.*, 2016; Bali & Gueddari, 2019). The substantial cost of these treatments and their complexity reduce the practicality of these techniques; therefore, cost-effective and highly efficient technology for phosphate removal gets great attention.

Table 2.2: Advantages of technologies used for phosphate removal from wastewater

Process	Advantage	Disadvantage
Adsorption	❖ Easy process operation ❖ Efficient at law phosphate concentration ❖ Low initial cost and by product (Siyal *et al.*, 2020)	The effect of co-existing ions selected against other contaminants
Biological processes	❖ Complete removal of phosphate. ❖ Low operation cost. ❖ Low amount of by-products (Huang *et al.*, 2017)	Ineffective in the removal of trace amounts of phosphate (Bacelo *et al.*, 2020)
Chemical precipitation	❖ Well developed & reliable process ❖ Achieve high phosphate removal (Kyong *et al.*, 2014)	•High chemical usage, sludge disposal & not effective at low concentrations
Physical processes	❖ High phosphate removal	High capital, energy and operational costs and poor selectivity ions

2.2. Adsorption

Adsorption is the collection or enrichment of chemical substances on a surface or interface. It is currently one of the most commonly used methods for treating wastewater. Adsorption is an easy operational technique that has been extensively and effectively used to remove contaminants, including phosphate, from aqueous solutions. Adsorption occurs between solid-solid, solid-liquid, solid-gas, liquid-liquid, or liquid-gas adsorbents and adsorbate substances, respectively (Sukmana *et al.,* 2021). It occurs when molecules, atoms, or ions from a gas liquid or dissolved solid adhere to a surface. The adsorption potential and mechanism of the contaminant depend on the adsorbent property (Tran *et al.,* 2019).

Usually, two central diving forces lead to the adsorption of solutes from an aqueous solution to adsorbents. The first driving force is associated with the solvent disliking (lyophobic) character of the solute in the adsorption system. A hydrophobic substance tends to be removed from the matrix solution. The second driving force is the electrical attraction of the solute to the solid, which occurs as a result of chemical interaction or Vander Waals interaction. The adsorption induced by the Vander Waals force is physisorption, and another type of adsorption is chemisorption. Physisorption is adsorption by van der Waals force, which is a weak intermolecular attraction that takes place below the critical temperature of the adsorbate and forms in the monolayer or multilayer (Xiong *et al.,* 2017). Chemisorption involves the transfer, exchange, or sharing of electrons between adsorbent and adsorbent (ions or molecules), and adsorption of adsorbate on adsorbent results in the formation of strong chemicals in an aqueous environment (Kong *et al.,* 2019).

Various adsorbents have been recommended for the recovery of phosphate from aqueous solutions, such as clay, zeolite, and carbon-based (Dai *et al.,* 2017). Activated carbon and its modified form have been widely utilized due to their exceptional properties, such as large specific surface area, abundant pore structure, chemical stability, ease of physical and chemical activation (Astuti *et al.,* 2019a), especially their properties for specific applications and ability to remove a variety of pollutants (Almanassra *et al.,* 2021). Adsorption techniques have various important parameters to evaluate their effectiveness, such as adsorbent dose, initial concentration of pH solution, and contact time.

2.2.1. Solution of pH

Solution pH has been designated as one of the most critical parameters for evaluating the adsorption process. It affects the degree of ionization of phosphate in solution, the surface charge of the adsorbent, and the dissociation of functional groups on the active site of the adsorbent. Protonation of the phosphate occurs at a pH range of 2 to 12, resulting in different species of phosphate ions such as H_3PO_4 and $H_2PO_4^-$ in the aqueous solution (Xiong *et al.*, 2017). At pH below 2, most of the time H_3PO_4 is dominant in the matrix solution. At this pH, phosphate removal is inhabited due to the presence of H_3PO_4 species, which interfere with the adsorption of other phosphate ions because of their stable structure. At a pH range between 2 and 8, species are the most dominant in aqueous solutions. The phosphate gets more protonated as the pH of the solution rises from 2 to 8, increasing the positive charge density on the adsorbent's surface. As a $H_2PO_4^-$ result, effective phosphate removal is observed at acidic pH levels (Fu *et al.*, 2020).

For phosphate, when the phosphate solution's starting pH rose from 3 to 6, the percentage removal of phosphate increased, but when the pH rose from 7 to 11, the percentage removal of phosphate decreased due to the presence of a number of hydroxide ions in the solution, resulting in a change in the adsorbent surface and inhibiting phosphate ions from reaching the adsorbing site on the adsorbent surface. Therefore, at lower pH, the percentage removal efficiency increased, whereas at higher pH, the phosphate removal efficiency decreased (Sakamoto *et al.*, 2020).

2.2.2. Adsorbent Dose

Adsorbent dosage is one of the critical parameters due to the adsorbent, which provides the binding sites for phosphate adsorption. Therefore, adsorbent dosage determines the capacity of the adsorbent for a given initial concentration, the separation cost, and thus the overall water purification process (X. Fan *et al.*, 2016). The percent of phosphate recovery is improved by increasing the amount of activated carbon. Thus, an increase in adsorbent particles is needed to ensure an adequate number of sites for phosphate ion adsorption (Ouakouak & Youcef, 2016). Therefore, the adsorbent's pore size and unoccupied site limit the rate and amount of phosphate molecules that can transfer to the surface.

2.2. 3. Concentration of Adsorbate

The adsorbate concentration is another factor that influences the adsorption process. With increasing starting concentration, removing potential can decline. At low concentrations, most phosphate ions may come into contact with the adsorbent's active sites, but as the concentration rises, all phosphate species will be unfavorable to contact the active surface due to strong competition.

2.2.4. Contact Time

Another critical parameter that has been discovered to have a major impact on the adsorption process is contact time. The required contact time varies between different adsorbents and contaminants. Generally, the adsorption of phosphate by most biomass-based activated carbon is reached at equilibrium below 3 hours in the removal process. Other research reports show that 3 hours were necessary for the removal of phosphate by coir pith activated carbon to reach equilibrium (P. Kumar *et al.*, 2010).

2.2.5. Effect of Competitive Ions

The co-occurrence of different ions in the phosphate solution affects the equilibrium adsorption capacity of phosphate with ACs. Commonly, wastewater, municipal, and industrial water streams consist of different ions that compete with each other on the adsorption sites. From those different ions, it is common to compete for phosphate adsorption using an adsorbent (A. Fetene *et al.,* 2022). Coexistence of those ions changes the pH of the solution and utilizes high affinity towards the active adsorption sites, which affect the phosphate adsorption capacity of phosphate onto AC. The effect of AC on phosphate adsorption was credited to the competition for the adsorption sites. The ionic radius of is very close to the ionic radius of phosphate and forms stronger bonds on both of the outer and inner sphere complexes, which makes them compete for the same adsorption, while the monovalent anions such as and form weaker bonds on the outer surface complexes with the vacant active sites (Almanassra *et al.,* 2020). For example, a 19% reduction in phosphate removal by thermally treated activated carbon was reported in the presence of a mixture of 0.016, 0.004, 0.053, and 0.013 mmol/g, respectively (Miyazato *et al.*, 2020).

2.2.6. Desorption

Elution is the most important approach to remediation adsorbate and recycling adsorbents. Usually, saline solutions and acidic solutions are considered popular desorbing agents, among others. However, the choice of the most fitting eluent depends on the desorption capacity, which is based on the recyclability of the application mechanism, the regeneration process, as possible damage to the adsorbent can occur with an ensuing loss in the adsorptive competence, and on economic and environmental aspects. From various types of tested desorbing agents, the research has been quite consistent in identifying sodium hydroxide (NaOH) solutions as the most appropriate ones. But chloride and sulfate solutions were not recommended as an efficient approach to the desorption of phosphate, which designates a strong bonding between the adsorbate and various adsorbents (Gu *et al.,* 2017; Nur *et al.,* 2014). For agricultural purposes, the direct use of the phosphate-loaded adsorbents can be considered an option. Köse and Kivanc suggested that, since phosphate is difficult to elute and the adsorbent composition is mostly phosphate-saturated, calcined waste eggshells may be used directly as fertilizers (Köse & Kivanç, 2011).

2.3. Activated Carbon

Black, solid, tasteless, microcrystalline, non-graphitic, and micro-porous forms of carbon known as "activated carbons" have a large surface area, well-developed pore structure, and pore volume that result from the thermochemical or thermal decomposition of carbon-based precursors in a limited oxygen environment. It is an important adsorbent due to its high adsorption capacity. As a result, it is used as an adsorbent for cleaning organic and inorganic pollutants because of its multifunctional properties, abundance of active sorption sites, stability, renewability, contaminant removal capacity, availability, high specific surface area, and high internal micro-porosity (Ambaye *et al.,* 2021; Singh *et al.,* 2020; Reyhanitabar *et al.,* 2020).

The adsorption characteristic of active carbon depends on the raw material type, size of the particle, and process used for production (P. Liu *et al.,* 2016; Salgado *et al.,* 2018). In addition, the adsorption capacity of the resulting AC is influenced by the activation reagent, activation time, impregnation ratio, pyrolysis temperature, and the presence of inorganic

impurities (Yahya *et al.,* 2015). It is used for various techniques of application, especially in wastewater treatment as an adsorbent by removing organic and inorganic pollutants (Sulyman *et al.,* 2017).

2.3.1. Structure of Activated Carbon

Pyrolysis temperature, type of starting material, and structure of the raw material are the major factors influencing the physiochemical properties of ACs, including surface area, functional groups, hydrophobicity, stability, and pH (Pariyar e*t al.,* 2020; Xiao *et al.,* 2018). In addition, the properties of the resulting activated carbon can also be affected by the type of activated reagents, time impregnation ratio, and inorganic impurities (Hirunpraditkoon *et al*., 2011; Patil & Kulkarni, 2012).

2.3.2. Physical Structure of Activated Carbon

Activated carbon is composed of three parts: amorphous carbon, single-plane rectangular carbon, and graphite microcrystal carbon. The microcrystalline activated carbon is different from graphite. Non-graphite microcrystalline structure makes activated carbon develop pore structure, and its pore structure can be characterized by pore size distribution (Jiang *et al.,* 2013). AC has relatively wide pore-purview dispersion in the range of 1nm to 100 nm. The occurrence of a large number of very fine pores (microspores) gives the AC a large inner surface, which is the basis for its special interest in many applications. A classification of the average width of pores is: micro-pores (2 nm), meso-pores (2–50 nm), and macro-pores (Abrha & Chen, 2017).

2.3.3. Chemical Structure of Activated Carbon

The structural structure of biochemical substances is associated with functional groups on the surface of activated carbon. These functional groups presented in Figure 2.1 on the surface ACs include (a) aromatic C-C stretching; (b) and (c) carboxyl-carbonates; (d) ring; (j) cyclic anhydride (6-membered-ring); (k) quinine; (l) phenol; (m) alcohol; and (n) ketene (carboxylic acid); (e) lactone (4-membered ring); (f) lactone (5-membered ring); (g) ether bridge; (h) cyclic ether; (i) cyclic anhydride (5-membered) (S. Wang *et al.,* 2020; H. Wang *et al.,* 2015; J. hong Zhang *et al.,* 2014). The number, type, and structural properties of these functional groups depend on the chemical and heat treatment of the carbon source. The

adsorption capacity of AC is influenced by both functional groups on the AC surface and its physical pore structure. The edge chemical bond of the aromatic skeleton that was created during the carbonization steps breaks to create an edge carbon atom with an unpaired electron during the production of AC. The initial carbon atoms can react with heterocyclic atoms like oxygen, hydrogen, nitrogen, and sulfur to generate various surface functional groups due to the existence of an unsaturated chemical bond. The functional groups on the surface significantly affect the adsorption properties of activated carbon (T. Li *et al.*, 2021).

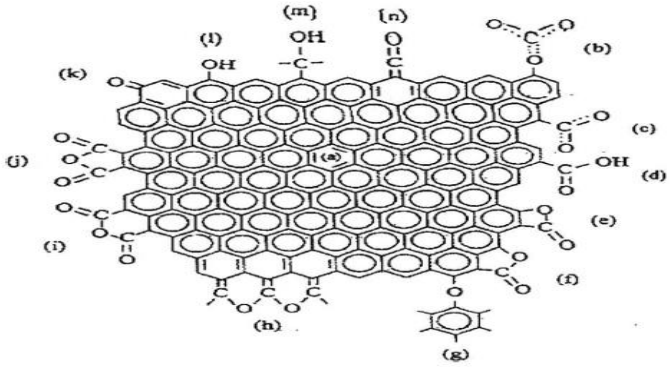

Figure 2.1: Functional group on activated carbon (Jabit, 2007)

2.4. Preparation Method of Activated Carbon

The preparation of AC from *Prosopis Juliflora* is proven to be a viable approach for controlling the species distribution, which is typically considered to be agricultural weed (Muthulakshmi Andal & Thangamani, 2016). A carbon-rich solid product called AC is produced by the thermochemical breakdown of biomass, which includes solid wastes like agricultural biomass such as Moroccan Jujube shells, wood, coconut shell, bamboo, jatropha husk, tamarind wood, sugarcane bagasse, shells, and manure, and *Prosopis Juliflora* (Kachabi *et al.,* 2019; Yusufu M. I., 2012; Chen *et al.*, 2012; Sahu *et al.*, 2010).

Preprocessing, carbonization, activation, and characterization are the major steps in the process of making PJAC (Malini *et al.*, 2023). Pyrolysis and activation in general are crucial for deserving high-quality AC. *Prosopis Juliflora* wood is preprocessed through chopping, grinding, washing, drying, and activation. PJ can be dried to eradicate moisture content using two techniques: oven drying, which is done in a hot air oven at 105 °C for 24 hours, and the sun-drying method, which is done by exposing the washed wet PJ to direct sunlight. The

objective of activation is to produce high-quality AC, and there are two techniques of activation for preparation of AC: physical and chemical activation (Wu *et al.*, 2019). Physical activation involves carbonization and activation in a single step or two separate steps at a higher temperature under the atmosphere of gasification gas (i.e., steam, carbon dioxide, nitrogen, or inert gas). The resulting AC has poor pore properties as compared to AC prepared from chemical activation. AC synthesis using chemical activation is performed in a single step at a lower temperature using precursor impregnated with chemical simultaneous heating (Tsai *et al.*, 2019) or two steps after the carbonization activation (Reza *et al*., 2020; Weber & Quicker, 2018).

2.4.1. Carbonization

Carbonization is the thermal decomposition of carbonaceous material. Usually, carbonization occurs at an optimal temperature in an inert environment to eliminate non-carbon species and volatile components and produce a fixed carbon mass. It is a complex process that includes dehydrogenation, hydrogen transfer, condensation, and isomerization. Pyrolysis of carbon-based materials creates a solid residue with high carbon content, often in an inert environment (Martínez De Yuso *et al.*, 2014).

Optimization of pyrolysis temperature in the range of 200–800 °C is usually used to manage the properties of ACs, depending on the type of feedstock. Increasing pyrolysis temperature results in an increase in carbon content, aromaticity, pH, ash content, surface area, stability, and pore size, whereas AC yield, hydrogen content, oxygen content, H/C, and O/C ratios decrease (Mukome *et al.*, 2013). The increased specific surface area of activated carbon is due to the release of numerous volatile substances from the biomass structure. However, parts of the porous structure can be collapsed at very high temperatures, and the pore will be blocked, which can reduce the active site of the adsorbent (Yin *et al*., 2018).

2.4.2. Activation Carbon

The purpose of activation is to create and develop porosity in the carbon material, thereby increasing the adsorptive capacity. Therefore, activation time, activation temperature, and heating rate are key factors for making ACs with particular characteristics (Domingues *et al.*,

2017). In principle, the methods for activating activated carbon can be divided into two types: physical and chemical activation.

2.4.3. Physical Activation

Two steps are involved in the physical activation of AC: (a) carbonization at low pyrolysis temperatures (400–750 °C) in the presence of heat, gases (carbon dioxide, helium, and nitrogen), and steam to break down the cross-linkages between the C atoms; and (b) activation in a gaseous environment at relatively high pyrolysis temperatures to increase the porosity of the AC. Various activating agents are reported in the literature, which include carbon dioxide, air, nitrogen, steam, and oxygen (Reza *et al.,* 2020). For the thermal activation of AC, mild oxidizing agents like steam and carbon dioxide are typically utilized because they encourage a delayed oxidation process that results in the development of new pores and the widening of existing pores (Contescu *et al.,* 2018). In the physical activation process, the main variables that determine the quality and distinguishing properties of AC are the activation time, temperature, and gas flow rate. According to Devi & Saroha's (2017) research report, AC surface area and porosity grow as gas flow rate and process temperature rise; however, activation time has adverse effects after a certain amount of time (Devi & Saroha, 2017).

2.4.4. Steam activation

Steam activation is a cost-effective technique for making AC that has a high porosity and surface area. In comparison to carbon dioxide activation method-produced AC, steam activation method-produced AC has higher adsorption efficiency and a wider range of pore sizes. The expansion impact of steam causes the mesopores of the AC to widen as a result of water molecules diffusing to the interior surface, increasing the BET surface area. However, if the activation temperature was higher than 800 °C, fixed carbon would be lost, which would reduce the amount of BET surface area (S. Wang *et al.,* 2017).

2.4.5. Carbon Dioxide, Nitrogen, and Air Activation

The functional groups of the AC are similarly impacted by carbon dioxide and nitrogen activation. Comparatively, the activation by nitrogen requires a significantly higher activation temperature, but the activation based on the use of carbon dioxide could enhance

the creation of micropores only at a lower activation temperature (600–800 °C) (Malini *et al.*, 2023). According to earlier research, the distortion of the acidic functional groups on the surface of biomass causes the acidity of the AC to drop and the basicity to increase as the activation temperature rises (Malini *et al.*, 2023). At 270–280℃, air activation of AC increases the surface with acidic oxygenated functional groups such as COOH and R-O-R-, which enhances AC's ability to adsorb (Bagreev & Bandosz, 2004).

2.4.6. Chemical Activation

Different chemical agents, like $ZnCl_2$, H_2SO_4, H_3PO_4, KOH, NaOH, K_2CO_3, $Fe(NO_3)_3$, and H_2O_2, are used in the chemical activation process (Devi & Saroha, 2017). The most popular and efficient activating agent for creating AC with a large surface area and greater adsorption capacity is potassium hydroxide. By removing the hydrogen and oxygen atoms from the PJ, potassium hydroxide acts as a dehydrating agent and triggers a condensation process, increasing the AC's surface area and pore volume. The adsorption efficiency of AC is affected as the impregnation ratio (IR) of reagents to precursors rises (Bhomick *et al.*, 2019). In addition, a rise in concentration slabs the AC's mesopores and microspores and reduces its surface area. The PJAC preparation process uses less energy since the potassium hydroxide activation method is effective in reducing the activation time and temperature. The BET surface area (500–1876 m^2/g) was reached as a result of the incremental impregnation ratio of potassium hydroxide to precursors. The surface area and adsorption effectiveness of AC are also influenced by the activation agent concentration (Masoumi & Dalai, 2020).

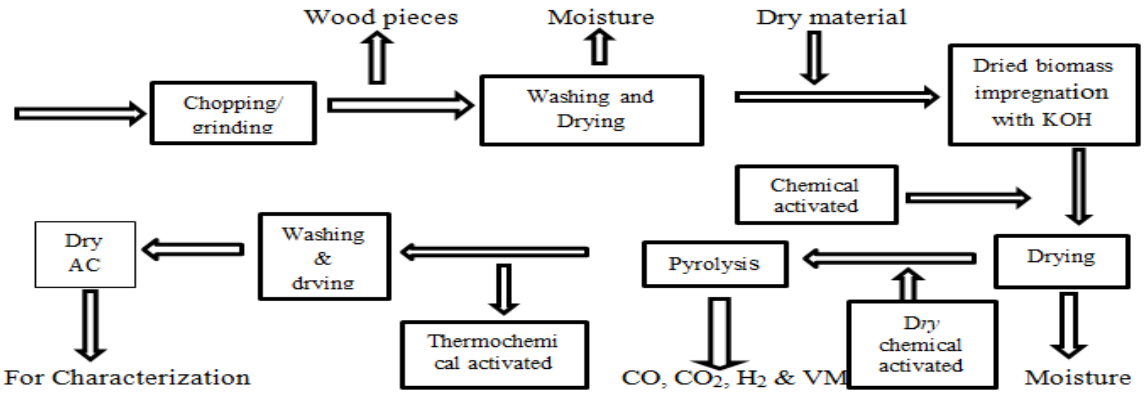

Figure 2.2: Flow diagram for preparation of AC (Reza *et al*., 2020)

Adsorption capacity and pore volume surface area both rise with concentration, but they decrease when activation agent concentrations are over the optimal level (Foo & Hameed, 2012). Figure 2.2 shows the flow diagram that can be employed to prepare AC from *Prosopis Juliflora* biomass.

2.5. Effect of activated carbon preparation

2.5.1. Pyrolysis Temperature

The characteristics and qualities of the PJAC are considerably affected by the temperature at which the pyrolysis of PJ is carried out. It has been shown that while the yield of AC falls as the pyrolysis temperature rises, the ash content increases (T. Wang *et al.,* 2020). Low-temperature AC is often yield-high in nature, whereas high-temperature AC is yield-lower. The outer surface appearance and structure of the PJAC are influenced by the pyrolysis temperature. Surface area and pore volume surface area both rises with optimal temperature. However, the AC's porosity was reduced beyond the optimal temperature, which also improved the smoothness of the surface structure and overall aromaticity (Colantoni e*t al.,* 2016).

2.5.2. Heating Time

Shorter heating times at high carbonization temperatures are reportedly necessary when pyrolyzing biomass (Pallarés *et al.,* 2018; T. Wang *et al.,* 2020). The recommended contact periods are 120 minutes at 500 °C (Marya *et al.,* 2020), and fast pyrolysis is done for a hardwood sample at a rate of 70 ml/min gas flow. The sample is heated at 35 ℃/min to 450 °C and then carbonized for 15 minutes. Other research showed the result of activated carbon derived from rice husk with a 1:3 (biomass: KOH) impregnation ratio by weight and activation at 750 °C for 1 h. It revealed the highest surface area and pore volume, 2138 m^2/g and 1.17cm^2/g, respectively (Juntakan *et al.,* 2021). According to Mohan et al. (2014), increasing dwell time at the same carbonization temperature resulted in a decrease in the micro-pore volume of AC (Mohan *et al.,* 2014).

2.5.3. Heating Rate

The primary factor that enables us to distinguish between the different forms of pyrolysis is the heating rate of PJ during pyrolysis (slow or fast pyrolysis). Heating rates on the order of

100 °C/min–100 °C/min are needed for slow pyrolysis processes, whereas heating rates of more than 1000 °C/min are needed for fast pyrolysis processes. Higher heating rates result in an increase in AC yield and carbon content while decreasing hydrogen content. The Colantoni et al. (2013) research report shows that the prolonged residence time during the carbonization process led to an increase in surface area with a decrease in heating rate (Colantoni *et al.,* 2016).

2.5.4. Effect of Impregnation Ratio

The impregnation ratio is defined as the ratio of the weight of the activating agent to the precursor. It is one of the most crucial factors in the chemical activation process. To enhance the adsorbent porosity with less activating agent usage, total saturation of biomass precursors must be ensured. As a result, fewer chemical substances are consumed, and the excess sample is better eliminated during the carbon washing procedure. The impact of a higher fraction of impregnation over a porous carbon structure is greater than that produced by a higher carbonizing temperature (Elmouwahidi *et al.,* 2017). Bhomick et al. (2019) found that the higher surface area and total pore volume were obtained with a ratio of 1:2 (Bhomick *et al.,* 2019). It is results in AC with increased surface area and total pore volumes. The increase in porosity was encouraged by the release of the tars and water gases that exist in the cross-linked structure due to the chemical reagents.

2.6. Application of Activated Carbon

Application of activated carbon Activated carbon is an organic, porous material resulting from the thermochemical transformation of biomass in a limited oxygen environment. It is a solid and carbon-rich material that can be used as an adsorbent agent because of its physicochemical properties, such as its high surface area and cation exchange capacity (Z. Xu *et al.,* 2019). Improves water holding capacity, retains the dissolved nutrients of water in the soil, decreases soil acidity, furnishes additional organic carbon and mineral nutrients, and enhances soil fertility by decreasing CO_2 and N_2O emissions (Guo *et al.,* 2020). Other soil and environmental benefits of activation are shown in Figure 2.3. AC can hold carbon for several years as well as reserving nutrients for the plant; this makes it more stable and effective than other organic matters used as fertilizers, such as compost and manure (M.

Amin *et al.*, 2022). In addition, AC has also been shown to enhance soil physical properties such as porosity, water holding capacity, and soil aggregate stability (Kavitha *et al.*, 2018).

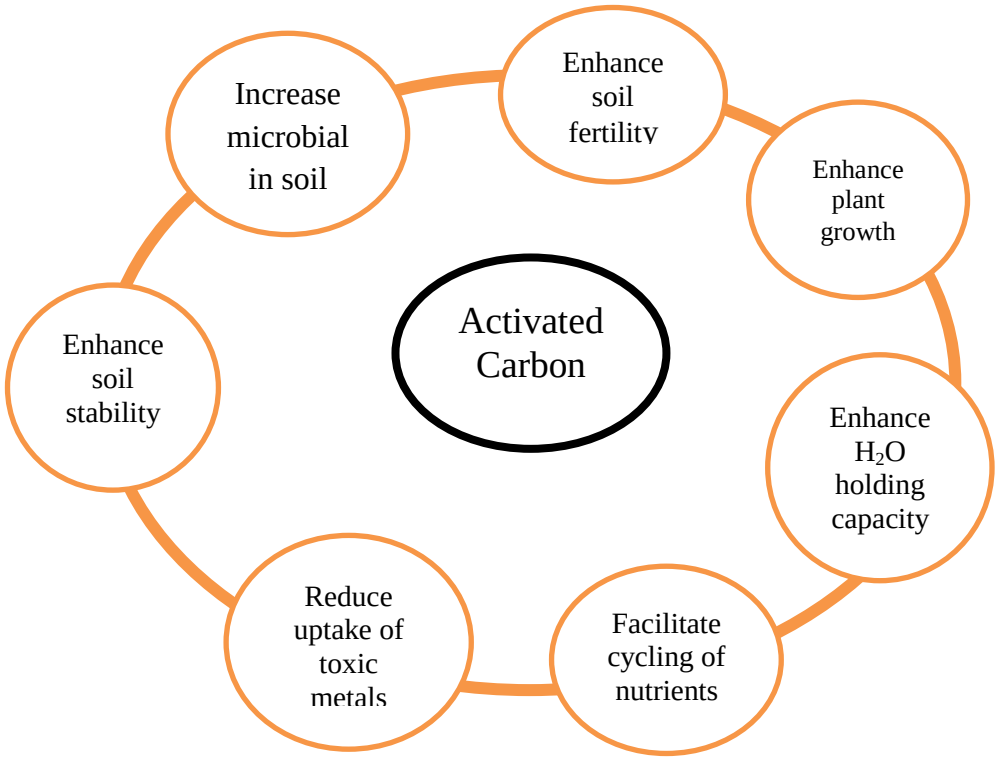

Figure 2.3: Capacity of activated carbon benefit in (Kavitha *et al.*, 2018; Rehman & Razzaq, 2017; F. R. Amin *et al.*, 2016)

3. MATERIALS AND METHODS

3.1. Materials

3.1.1. Chemicals and Reagents

All chemicals and reagents used in this study were analytical grades. Potassium hydroxide, KOH (LOBA CHEMIE PVT.LTD, 98%), Potassium dihydrogen phosphate, KH_2PO_4 (LOBA CHEMIE PVT.LTD, 98%), Hydrochloric acid, HCl (LOBA CHEMIE PVT.LTD, 37%) were used for chemical activation of the activated carbon (AC), and Sodium Hydroxide, NaOH (LOBA CHEMIE PVT.LTD, 98%), was used for pH adjustment and desorption and potassium chloride, KCl (LOBA CHEMIE PVT.LTD, 99%) was used as electrolyte for determination of point of zero charge (pHpzc) of adsorbent. In addition nitric acid, HNO_3 (LOBA CHEMIE PVT.LTD, 68%) and detergents were used for cleaning and distilled water was used to prepare solution and to rinse equipment.

3.1.2. Apparatus and Equipment

The apparatus and equipment used for characterization of adsorbents during this study were, X-ray diffractometer (XRD) (XRD-7000, Japan), Fourier Transform Infrared Spectrometer (FTIR) (mode FT/IR6600, Japan), Scanning Electron Microscope (SEM) (JCM-6000PLUS Bench Top SEM, JEOL, Japan), Brunauer–Emmet–Teller (BET) (SA-9600, USA), and UV-Vis spectrometer (UV-Vis-2000 AUG, USA). Analytical balance (FA-2014 GERMAN), Muffle furnace (MF-2014, Germany), pH (pH7110, Germany) and conductivity meter (Cond7110, Germany), Oven (UF260), Orbital shaker (OS-500OS) were used for different activity.

3.2. Methods

3.2.1. Sample Collection

The wastewater samples were collected from Metehara Sugar Factory (MSF) municipal wastewater discharging point. Methara is found in Easter show, Oromia Regional State, Ethiopia. It is located 8°54'0"N and 39° 55'0"E and 200 km from Addis Ababa. MSF is one of the older sugar producer factories in Ethiopia. Most Sugar industries located near to where the raw material (sugarcane) grows. Moreover it uses intensive human power, resulting installation of homes, hospital and schools around the factory to give facility for the

employee. MSF accumulates more than ten thousand households. From these installed residences produce large amount of wastewater and then directly discharged to Awash River without ant treatment. Composite wastewater sample was collected from discharging points of using plastic bottles; sample volume of 1L was collected. The bottle used for collecting wastewater samples was earlier washed carefully with HNO_3, with detergent, rinsed distilled with water and saturated with wastewater sample at the point of collection. Sample collection, preservation and storage were performed according to standard procedures recommended by United State Environmental protection Agency (USEAP) guide to water sample. We used composite samples collected four timed per day at 3 hours of interval. The physiochemical parameters of municipal wastewater sample including: temperature. color, pH, electrical conductivity, soluble ions (Cl^-, CO_3^{2-}, NO_3^-, SO_4^{2-} and phosphate) and COD were conducted based on standard method of analysis (Brandi & Wilson-Wilde, 2013).

3.2.2. Preparation of Phosphate Solution and Working Solution

At room temperature, 0.439 g of potassium dihydrogen phosphate, KH_2PO_4 was added to distilled water to prepare stock solution of $100\ mgL^-$ in 1000 mL volumetric flask. The standard series solutions were prepared from previously prepared stock by using dilution methods. UV- Vis spectrometer was used to measure the concentration of phosphate from solution at the maximum absorbance of λ_{max} 880nm (Astuti *et al.*, 2019a).

3.2.3. Adsorbent Preparation

The wood part of *Prosopis Juliflora* was collected from KSF cane field, in Afar regional State, in Ethiopia. It is located at 9°26'0"N and 40° 30'0"E and 74 km away from MSF, 270km from the capital Addis Ababa, near the main road of Addis Ababa-Djibouti. The sample was collected using composite sampling method from similar species and from different parts wood. The wet wood part of the sample was chopped into 5 mm, washed using distilled water and dried in oven for 24hs at 110℃. The oven dried raw material *Prosopis Juliflora* was grinded using laboratory mill, and sieved to obtain optimal size 150 µm sieved material of PJ was impregnated with pellets Potassium hydroxide (KOH) at ratio of 1:1 (Hui & Zaini, 2015). The impregnated process was allowed to sit for overnight to keep chemical reagent to be fully adsorbed to the raw material. The impregnated material was dried in oven

at 105℃ for overnight to eliminate extra moisture entirely. Finally, the oven dried sample was stored inside an air-tight plastic bag and subjected to the process of pyrolysis.

The oven-dried PJ samples were carbonized at temperature 400℃, 500℃ and 600℃ for 120 min (Reza *et al.,* 2020). The muffle furnace temperature was programed at rate of 10℃ per min, and then the produced PJAC was cooled for 24 hr. in dissector. The PJAC was washed using 0.1N HCl and distilled water till pH attains 7 to remove any remaining ions and impurities and dried at 105℃ in an oven to constant weight. Then dried PJAC was grinded and sieved through 150 µm sieve to attain sample particles size carbon based adsorbent labeled as PJAC400, PJAC500 and PJAC600. Then PJAC sample was stored in inside air-tight plastic bag.

3.3. Physiochemical Analysis of Activated Carbon

The physiochemical characteristics of PJAC400, PJAC500 and PJAC600 analysis were conducted in Ethiopian sugar industry Group (ESIG) research laboratory.

3.3.1. Moisture Content

The moisture content PJAC400, PJAC500 and PJAC600 samples were determined by the weight loss of the sample as it was heated to 105℃ (ASTM D3173, 1994). The moisture content of the sample calculated using equation

$$\text{Moisture\%} = \frac{W_1 - W_2}{W_1} \times 100 \quad \text{..... Eq. 2}$$

where, $w_1 and w_2$ the weight of sample before and after drying (gm), respectively

3.3.2. Ash Contents

Ash content of PJAC400, PJAC500 and PJAC600 samples were determined by tacking 1g dried sample individual and then incinerated at temperature 800℃ for 180 mints. The crucible was cooled in dissector and reweighed (ASTMD2866, 1994). The percentage of ash content was evaluated by equation 3.

$$\text{Ash\%} = \frac{W_2}{W_1} \times 100 \quad \text{.....Eq. 3}$$

where, $w_1 and w_2$ the weight of sample before and after incineration (gm), respectively

3.3.3. Volatile mater

For volatile mater determination of the PJAC400, PJAC500 and PJAC600 samples, about 1 g of dried sample was weighed and incinerated at 950℃ for 7 min in muffle furnace. The crucible cooled in desiccator and reweighed. The percentage of weight loss was considered as percentage of volatile mater (ASTM D3175, 1994). The volatile mater was calculated using equation 4.

$$\text{Volatile mater (\%)} = \frac{W_1 - W_2}{W_1} \times 100 \quad \text{..... Eq. 4}$$

Where, $w_1 and w_2$ the weight of sample before and after incineration (gm), respectively

3.3.4. Fixed carbon

The fixed carbon content of PJAC400, PJAC500 and PJAC600 was calculated, and it is the result of summation of percentage of moisture content, ash content and volatile matter content subtracted from 100. The fixed carbon content was calculated using equation 5.

$$\text{Fixed carbon (\%)} = 100 - ((Moisture(\%) + Ash(\%) + (Volatile\ matter(\%)) \quad \text{..... Eq. 5}$$

3.3.5. AC yield

The yield of AC is one of the important parameters to evaluate the efficiency of AC preparation methods. The yield of PJAC was determined as the ratio of the weight of the produced PJAC to the impregnated sample of dried weight subjected to pyrolysis. PJAC was calculated using equation 6.

$$\text{Yield}_{\text{PJAC}} = \frac{\text{mass of PJAC(gm)}}{\text{mass of dried PJ(gm)}} \times 100 \quad \text{..... Eq. 6}$$

3.5.6. Bulk density

The bulk density was evaluated by insertion of 5 gm of PJACs in a 10 ml graduated cylinder to a volume of 3-4cm^3. Then, the cylinder was tapped against a hard surface about 50 times to "compact" the PJAC and the volume (cm^3) was read (ASTMD2866-94. 2014). The bulk density was calculated using equation 7.

$$\rho = \frac{M_S}{V_b} \quad \text{..... Eq. 7}$$

where, ρ is the bulk density (g/cm^3), M_S is mass (g), V_b is the volume of the sample in cm^3

3.4. Structural Characterization of *Prosopis Juliflora* Activated Carbon

The adsorption rate is related to adsorbent type and highly depends on characteristics of adsorbents. In this study, structural characteristics off adsorbent were studied by detecting FTIR, XRD, SEM, BET and pH_{pzc} (Thongpat et al., 2021; Marya *et al.*, 2020)

3.4.1. Fourier Transform-Infrared Spectroscopy (FT-IR) analysis

FT-IR technics was used to qualitatively estimate the functional groups of the surface PJAC pyrolyzed at different temperature. FT-IR spectroscopy (model FT/IR6600, Japan) recorded spectra in wave length in the range of 400-4000 cm^{-1} using potassium bromide (KBr) pellet method. For FT-IR characterization, 1gm of sample and 100 mg of KBr were mixed with mortar and pestle. Small amount of powder from the mixture was pelletized using mechanical presser. Finally, the pellet was analyzed using FT-IR spectroscopy to determine the functional group of the adsorbent (Banik *et al.*, 2018). In this study FT-IR analysis result of PJAC pyrolyzed at different temperature were considered as one of parameter to be selected in pyrolysis of PJAC.

3.4.2. X- ray Diffraction (XRD) analysis

XRD patterns PJAC400, PJAC500, PJAC600 and APJAC500 were documented using an X-ray diffractometer (XRD700, Japan) in Jimma Institute Technology (JIT) at department of Material Science and Engineering to evaluate the amorphous and crystalline nature of adsorbent. Same amount of adsorbent sample was taken for each adsorbent from previously prepared sample and field in a sample holder. Then, the sample was analyzed by using an X-ray diffractometer with Cu-Kα radiation source $\lambda = 1.54$Å and operating 40kv and 30mA. X-ray diffractograms were obtained for 2θ angles scan range from 10° to 80° with scan step 0.02° and scan speed of 3° at rating time of 0.40 sec.

3.4.3. Scanning Electron Microscope (SEM) analysis

The PJAC400, PJAC500 and PJAC600 adsorbent surface morphology were studied by SEM (JCM-6000PLUS Bench Top SEM, JEOL, Japan) using a high-energy electron and out coming electrons are analyzed by applying a 10 K electron acceleration voltage. For SEM analysis 30 mg sample were taken from prepared sample and characterized by SEM were resulting image gives information about the surface nature and textural, shape, size and

arrangement of the particle on the sample's surface. The analysis was done in Adama Science and Technology University (ASTU).

3.4.4. Brunauer-Emmet- Teller Analysis

The surface area of PJAC500 was determined by using the BET instrument (SA-9600 Series Surface Area Analyzer) (SA-9600, USA) in Addis Ababa Science and Technology University at department of Chemical Engineering. For BET analysis, empty sample holder was weighed using analytical balance and 0.1 g sample was placed in empty sample holder. Then, sample was degassed at temperature of 300 ℃ for 9 h to remove impurity from the sample in the degas station of surface area analyzer according to the International Union of Pure Applied chemistry (IUPAC). From degassed sample 0.05 g placed in analysis station in the range of 0.1 to 0.99 relative pressures and 10 Psi of Nitrogen gas.

3.4.5. Point of Zero Charge (pH_{pzc}) Analysis

The Point of Zero Charge (pH_{pzc}) adsorbent was measured by mixing of 0.1g PJAC sample produced from *Prosopis Juliflora* wood with 50 mL of 0.1M NaCl solution at different initial pH (2-12). The initial pH of the mixture was adjusted the range using either 0.1NM HCl or 0.1N NaOH solution. Each flask was agitated using orbital shaker for 24 hr. at room temperature. The pH of the liquid supernatant was then measured using pH meter. As a result, the pH difference between each solution's initial and final pH (pH_f -pH_i) was calculated and plotted against the initial pH value. Therefore, the initial pH at which ΔpH is zero is the pH_{pzc} (Dim *et al.,* 2021).

3.5. Bach Adsorption Experiment

Many adsorption experiments were conducted in batch model due to its simplicity and practicability technology in small scale determination (Astuti *et al.,* 2019a). For each parameter Batch model adsorption experiments were performed in 200 mL polyethylene for each parameter by adding specified amount of adsorbent and mixes with 100 mL of phosphate solution and adjusting the pH solution using 0.1M HCl and 0.1M NaOH. The sample was then stirred on orbital shaker at rate of 200 revolutions per minute (rpm) for specific time. After agitation, the adsorbent was filter by using of Whatman No 42 filter paper. The concentration of phosphate was determined by using UV-Vis spectrophotometer

(UV-Vis 200 AUG, USA) by Ascorbic- molybdate method at maximum wave length of 880 nm (Astuti *et al.,* 2019a). Then, the percent of adsorption efficiency (%R) and the adsorption capacity (mg/g) of adsorbent were calculated using Equation 8 and 9 respectively.

$$\%R = \left(\frac{C_0 - C_f}{C_0}\right) \times 100 \text{ ……..... Eq. 8}$$

where, %R is percent removal, C_o is initial concentration P and C_f is concentration after adsorption

$$q_e = \left(\frac{C_0 - C_e}{m}\right) V \text{…… Eq. 9}$$

where, q_e is the P quantity adsorbed at equilibrium (mg/g), C_o is the initial concentration of P (mg/L), C_e is the equilibrium concentration in solution after adsorption, m is adsorbent mas in gram and V is volume of P solution (L)

3.5.1. Effect of Solution Temperature

The effect of temperature toward adsorption efficiency of PJAC was studied by varying the solution temperature and keeping other variable constant. The temperature of 20℃, 25℃, 30℃ 35℃, 40℃and 45℃ was taken based on study report (Zhou *et al.,* 2019). 4 g/L of adsorbent as added to 100 mL volume of 25 mg/L phosphate solution for 180 minutes contact time at rate 200 rpm at pH 4. After the completion experimental process, the filtrate concentration of phosphate was analyzed using UV-Vis spectrophotometer.

3.5.2. Effect of pH

The solution's pH has a capacity to change the surface of adsorbents, thus influencing its adsorption potential (Almanassra *et al.,* 2021). Therefore, it is crucial parameter to investigate any adsorption experiments. By varying the solution pH (2, 4, 6, 8, 10 and 12) while keeping other parameters constant, the influence of initial pH on the removal of phosphate from an aqueous solution was studied by using 0.4 g KPJAC adsorbent was added to 100mL volume 25mg/L phosphate solution and agitated for 180minutes on shaker at temperature of 30℃.

3.5.3. Effect of Adsorbent Does

Activated carbon in varying amount was added to polyethylene tube containing constant phosphate solution. The effect of adsorbent dosage was studied using 0.1, 0.2, 0.3, 0.4, 0.5 0.6, 0.7 and 0.8 g of PJAC in 200 mL polyethylene tube with phosphate concentration 25 mg/L. Adsorbent does (0.1, 0.2, 0.3, 0.4, 0.5, 0.6, 0.7 and 0.8 g) was selected based on literature (Ouakouak & Youcef, 2016) and evaluated by keeping other parameter constant. Finally, the residual phosphate concentration which remains in filtrate was measured by UV-Vis spectrophotometer.

3.5.4. Effect of Initial Concentration

This parameter determines the effect of adsorbate concentration on its removal efficiency. 0.5 g of adsorbent placed in polyethylene tube with 100ml volume phosphate solution. The impact of phosphate concentration was assessed using phosphate concentration of 5, 10, 15, 20, 25, 30, 35 and 40 mg/L. The initial concentration range was selected based on literature reported that the concentration of phosphate present in wastewater in the above range (Y. Fetene & Addis, 2020). The pH was adjusted at pH 4, the contact time of experiment was fixed at 180 minutes and stirring rate was 200 rpm at room temperature.

3.5.5. Effect of Contact Time

Contact time is one of an important parameter for studying practical application of the adsorption process. For determination the impact of contact time 0.4 g of adsorbent was added to 100 mL volume 25 mg/L phosphate solution was added for various contact time (30, 60, 120, 180, 240, 300, 360 and 420 minutes) while other parameter were kept constant. The contact time was selected and studied based on the literature reported by (Astuti et al., 2019a) finally, the residual phosphate concentration which remains in the filtrate was measured by UV-Vis spectrophotometer.

3.6. Equilibrium Isothermal Modeling

Isotherm Equilibrium with parameter corresponding to surface characteristics and affinity of adsorbent were used to describe the equilibrium adsorption data which provide information about the capacity adsorbent (Ragadhita *et al.,* 2021). The adsorption isotherms were

generated based on theoretical models of adsorption such as: Langmuir and Freundlich models of adsorption isotherms.

a. Langmuir Adsorption Isotherm

The Langmuir adsorption isotherm model as performed since it assumes that adsorbate attach to homogeneous active site in monolayer, attaining saturation. This model also assumes that there is no interaction between the adsorbed molecules on adjacent site (Fito, Said, *et al.*, 2019). The Langmuir model can be represented by equation 10.

$$\frac{C_e}{q_e} = \frac{1}{q_{max} K_L} + \frac{1}{q_{max}} C_e \quad \text{..... Eq. 10}$$

The separation factor (RL) whose value determines the nature of isotherm shape is an important feature of Langmuir isotherm. It represent favorable ($0 < R_L < 1$), unfavorable ($R_L > 1$), liner ($R_L = 1$) or irreversible ($R_L = 0$) (Najmi e*t al.*, 2020). Separation factor (R_L) calculated using equation (11).

$$R_L = \frac{1}{1 + K_L C_o} \quad \text{..... Eq. 11}$$

b. Freundlich Adsorption Isotherm

Freundlich isotherm model is an empirical relationship describing of solutes from a liquid to solid surface and used for multilayer, heterogeneous adsorption site (Rajahmundry *et al.*, 2021). The Freundlich adsorption model is represented by equation 12.

$$\log q_e = \log K_f + \frac{1}{n} \log C_e \quad \text{..... Eq. 12}$$

Where, C_e is the equilibrium concentration of phosphate (mg/L), q_{max} is the maximum monolayer adsorption capacity (mg/g), q_e is equilibrium adsorption capacity (mg/g) and K_L is the Langmuir constant (L/mg), C_o is the maximum initial phosphate concentration (mg/L), K_f is Freundlich constant and $\frac{1}{n}$ is an empirical parameter related to adsorption intensity.

3.7. Adsorption of Kinetic Model

The rate of the adsorption process and the possible rate studying phase were examined using kinetic model (Maki & Qasim, 2023; Narvekar *et al.*, 2021). The linear forms of pseudo-first-order and pseudo-second-order kinetic model were applied in this study to give insight into mechanisms controlling phosphate adsorption on AC. The kinetic studies were conducted

using 100 mL aqueous solution of 25 mg/L phosphate and 0.5 g does AC added into 100 mL polyethylene tube.

a. Pseudo-First-Order Kinetic Model

The next equation presented the linear form of pseudo-first-order kinetic model. The adsorption rate $k_1$was calculated from linear regression analysis from the slop of linear plot of experimental data $\log(q_e - q_t)$ Vs t. Pseudo-first-order kinetic model designated by equation 13.

$$\log(q_e - q_t) = \log q_e - \frac{k_1 t}{2.303} \quad \text{..... Eq. 13}$$

b. Pseudo-Second-Order kinetic model

Pseudo-second-order kinetic model is probably the most widely used for adsorption kinetic (Bullen *et al.*, 2021). The linear form of pseudo- first-order can be expressed by equation 14.

$$\frac{t}{q_t} = \frac{1}{K_2 qe} + \frac{1}{q_e} t \quad \text{..... Eq. 14}$$

Where $K_1(min^{-1})$ is the capacity of pseudo-first-order adsorption rate, K_2 $(gmg^{-1}min^{-1})$ is the pseudo-second-order rate, q_e is the adsorption capacity of equilibrium and q_t is the adsorption capacity at time t.

4. RESULT AND DISCUTION

4.1. Characteristics of *Prosopis Juliflora* Activated Carbon

4.1.1. Physiochemical Characteristics

The physiochemical characteristics of PJAC carbon were evaluated according to American standard test method (ASTM, 2004) and the data were presented in the table 4.1.

Table 4.1: Physiochemical property of *Prosopis Juliflora* activated carbon (PJAC)

Parameter	Pyrolysis temperature(℃)		
	400	500	600
Moisture content (%)	5.47 ± 0.36	4.30 ± 0.3	3.78 ± 0.24
Volatile mater (%)	69.63 ± 0.56	65.27 ± 0.5	63.85 ± 0.42
Ash content (&)	3.26 ± 0.12	4.05 ± 0.05	4.93 ± 0.34
Fixed carbon (%)	22.64 ± 0.26	26.38 ± 0.21	27.44 ± 0.19
Yield (%)	55.37 ± 0.54	51.73 ± 0.63	48.25 ± 0.45
Bulk density (g/cm 3	0.87 ± 0.012	0.81 ± 0.01	0.74 ± 0.011

4.1.1.1. Moisture Content

The moisture content of precursors directly affects the carbonization time and carbonization temperature. The existing moisture in prepared activated carbon was evaluated to find out its

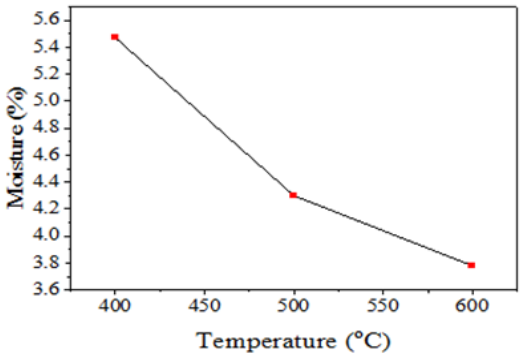

Figure 4.1: Effect of carbonization temperature on moisture

suitability in adsorption experiments using equation 2. In Table 4.1 presentation shows that the results specify an increase in activation temperature from 400°C to 600°C with impregnation ratios of 1:1 for PJAC; the moisture content of the prepared activated carbon

samples reduced. As Figure 4.1 shows, it was observed that as the activation temperature increased, the moisture content in activated carbon samples decreased (Arthi *et al.*, 2019). This result may be linked to removing volatile matter, thereby reducing carbon yield and simultaneously reducing the moisture content in the prepared PJAC samples. Similar study report, the AC prepared from *Bambusa vulgaris striata* using KOH activation is indicate consists of the result (Marya *et al.*, 2020).

4.1.1.2. Ash Content

Ash content is inorganic impurities which is white substance after PJAC has burned completely at high temperature (900℃). In this study the ash content of the materials is presented in Figure 4.2. The results described that increasing carbonization temperature from 400 to 600°C for prepared AC ash content increased from 3.26% to 4.93 %. This result is in agreement with the research conducted by (Juntakan *et al.*, 2021). Increased ash content can occur due to the formation of mineral salts present in PJ which if continued will form fine particles of the mineral salt. This is due to the mineral content contained in the biomass starting material for carbon making. As Figure 4.2 shows mineral material will then form into an ash compound when the oxidation process is carried out.

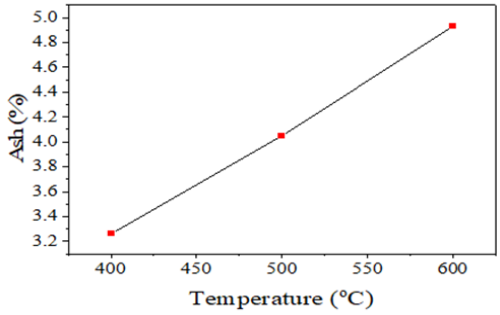

Figure 4.2: Effect of carbonization temperature on ash contents

4.1.1.3. Yield of PJAC

Yield of PJAC defined as the weight ratio of the resulting activated carbon to that of the pretreated PJ biomass. The carbon yield results for the prepared PJAC show that as carbonization temperature rising from 400°C to 600℃ as presented in Figure 4.3. The results showed that increasing activation temperature decline the percentage of PJAC yield: the result is related with promoting carbon burn-off and volatilization of tar at elevated temperatures. The weight loss is due to formation of volatile gaseous molecules like CO_2 and

CH_4 accompanied by bio-oil production with an increasing activation temperature. Similarly, the decrease in carbon yield could be attributed to the potassium hydroxide impregnation, which might be promotes escaping of volatiles from the sample resulting in the decrease in carbon yield. The reduced carbon yield related with impregnation may be due to the enhancement of carbon burn-off by activating agents. Similar study was reported in the literature by researcher who worked on preparing activated carbon from Agro waste biomass (Njewa *et al.*, 2022) confirms the obtained result.

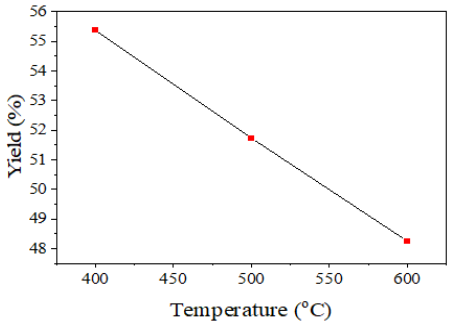

Figure 4.3: Effect of carbonization temperature on yield

4.1.1.4. Volatile Matters

Volatile matters is increase in activation temperature from 400°C to 600°C resulted in decreases of volatile matter from 69.63 to 63.85% as shown Table 4.1. The results showed that increasing carbonization temperature caused a decrease in the volatile matter content in PJAC. The reduction in the volatile matter percentage as activation temperature increases is connected to the fact that more volatile matter is released at an elevated temperature, lowering its content in prepared activated carbon (Ngueabouo *et al.*, 2022; Ramli *et al.*, 2021). This may be due to the increasing temperature resulted in further cracking of the volatile fractions into low-molecular-weight liquids and gases. Activation temperature has an influence on the structure of AC due to the release of volatiles and the formation and volatilization of intermediate melts (Juntakan *et al.*, 2021).

4.1.1.5. Fixed Carbon Content

The carbon content in derived activated carbon samples was calculated. At given impregnation ratios and elevating activation temperature from 400°C to 600°C for 2 hr., the carbon content for the prepared AC samples decreased as shown in Table 4.1. The fixed

carbon content results depend on the percent of volatile matter, ash, and moisture content. The results specified that an increase in activation temperatures promotes the release of volatile matter and increases the ash content while at the same time decreasing the moisture content. The obtained result confirm with Njewa et al (2022) study report (Njewa *et al.,* 2022).

4.1.1.6. Bulk density

The bulk density of PJAC derived at different pyrolysis temperature shows a decreasing tendency in value as pyrolysis temperature increase. As pyrolysis temperature increases from 400 ℃ to 600 ℃ the bulk density decline from 0.87 g/cm^3 to 0.74 g/cm^3 as Table 4.1 shows. The results confirmed, the PJAC that is used in this study is judged to provide a good adsorption capacity. Low bulk density and an increase in porosity encourage adsorption; means the adsorbent has comparatively large capacity of adsorbing the adsorbate (Jjagwe *et al.,* 2021).

4.1.2. Surface Area Analysis

BET surface area is one factor that affects adsorbent capacity for adsorption. *Prosopis Juliflora* adsorbent prepared in this study, have surface area of 554.143 m^2/g. Manjunath and Kumar (2018) study report shows that PJAC prepared from PJ biomass with absent chemicals reagent activation activated at similar temperature carbonization has surface area of 358.47m^2/g (Manjunath & Kumar, 2018). It can be seen that the specific surface area the prepared KPJAC500 higher than that of PJAC. This is because impregnation with potassium hydroxide resulting an increasing of specific surface area. The pore structure of ACs was mainly developed by volatile contents release, gasification and reaction of oxide derived from KOH with carbon atoms.

The degree of adsorption is directly related to the specific surface area, where the large the surface area the greater the surface for adsorption to take place (Jiang *et al.,* 2019; Ambroz *et al.,* 2018). In this way the adsorbent prepared in this study have promising performance in removing phosphate from solution than the heat treated PJAC. Based on this different activated carbons derived from agricultural biomass have been compared in Table 6.1 on index B with the prepared activated carbon in this study.

4.1.3. X-ray Diffraction

XRD analysis was carried out for identification of crystalline nature of the materials. Figure 4.4 illustrate X- ray diffraction pattern of the prepared activated carbons; KPJA400, KPJAC500, KPJAC600 and AKPJAC500. The diffraction of the four samples shows the same appearance with diffraction peak respectively $2\theta = 23°$ and $2\theta = 43°$ which shows the predominately amorphous structure (Moi *et al.*, 2018). The existence of the bump the high degree of disorder observed on the diffractograms of carbons is a characteristic of carbonaceous materials. Similar structures have also been reported by other researchers who prepared activated carbons from different lignocellulose raw materials (Mistar *et al.*, 2018).

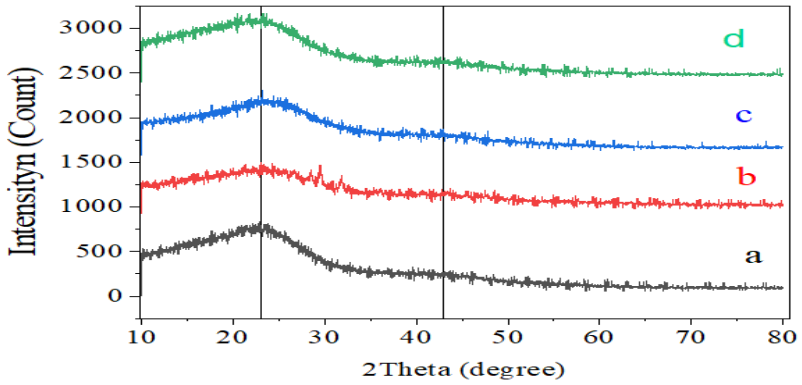

Figure 4.4: XRD pattern for (a) KPJAC400 (b) KPJAC500 (c) KPJAC600 and (d) AKPJAC500

4.1.4. Functional Group Determination

The functional groups exist on the adsorbent surface was evaluated using FT-IR, and a molecule's spectra are considered to be important property (Heidari *et al.*, 2014). FTIR of KPJAC400, KPJAC500, KPJAC600 and phosphate loaded KPJAC500 are shown on Figure 4.5. As shown in Figure 4.5a-d, a peck vibration formed between 3700- 3200 cm^{-1} which assigned by line in this study designated for $-$OH stretching (Marya *et al.*, 2020), which indicated compounds of phenols, alcohols, and hydroxyl groups (Malhotra *et al.*, 2018). The peak increased as the carbonization temperature rise from 500℃ to 600℃, indicate that large number of free and related hydroxide bond structure of hydroxyl (-COOH and COH) and associated with water, alcohol and carboxylic functional groups were decomposed in pyrolysis (Saka *et al.*, 2012; Üner & Bayrak, 2018). Due to the presence of the amino group's

N-H stretching vibration around 3440 cm^{-1}, it overlaps with OH stretching, resulting in a broader peak (Tang *et al.*, 2017). The peak at approximately 2927 cm^{-1} and 2855cm^{-1} were generated by asymmetrical and symmetric -CHx stretching vibration, showing that the aliphatic structures existed in PJAC. A peak at around 2360 cm^{-1} assigns the presence of $C \equiv C$ (alkynes) stretching vibration (Marya et al., 2020). The KPJAC400 and KPJAC500 bands at 1505–1580 cm^{-1} respond to aromatic annulus stretching (C=C) which are due to the existence of acids, aldehydes and esters in PJ (Lu *et al.*, 2013; Yacob *et al.*, 2017). The presence of the C–O stretching group in acids, alcohols, phenols, ethers, and esters can be recognized between peaks of 1407 cm^{-1} and 1058 cm^{-1} (Labied *et al.*, 2018). The peak detected at 1052cm^{-1} is associated with the ant symmetric stretch of C-O-C (Njewa *et al.*, 2022). The peaks from 579 cm^{-1} to 875 cm^{-1} are indorsed to the -OH and -CH out-of plane bending vibrations and C–C stretching (Marya *et al.*, 2020). The peaks band between 600–800 cm^{-1} recognized to the existence of aryl and heterocyclic aromatic components, which were mainly unchanged, indicating that the aryl C groups were fairly stabilized in pyrolysis (Lu *et al.*, 2013). The reservation of the structure suggests the creation of condensed aryl structure in prepared KPJAC (X. Wang *et al.*, 2021). The bonds below 600 cm^{-1} which are

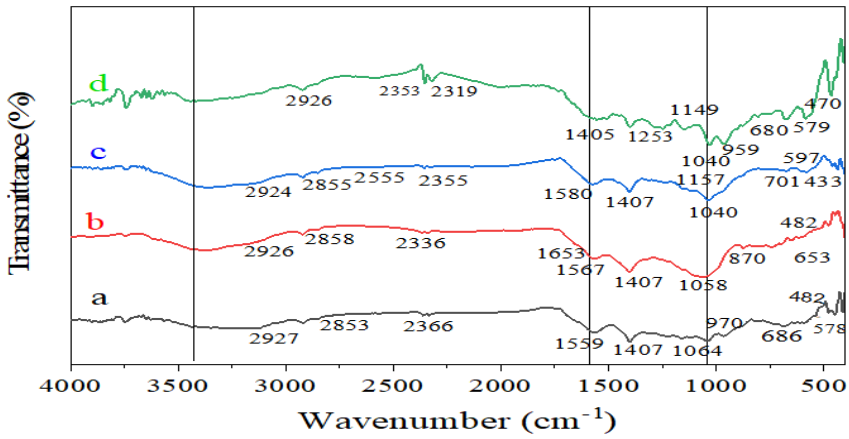

Figure 4.5: FTIR spectra for (a) KPJAC400 (b) KPJAC500 (c) KPJAC600 and (d) AKPAC500

mainly seen for KPJAC at carbonization temperature of 400℃, 500℃ and 600℃ were induced by metal–halogen (M–X, M for metal and X for halogen) stretch vibration, which is the primary feature between the FTIR spectra of AC derived from plant materials (J. hong

Zhang *et al.*, 2014). The peak between 600 and 1000 Cm^{-1} could be consigned to metal oxygen bonds (Chandradass *et al.*, 2010). The detected changes that occur on the AC surfaces prepared at different pyrolysis temperature confirmed influences of pyrolytic temperatures on the conversion of functional group types. This includes the transformation of one functional group to another, decomposition of existing functional groups in the precursors, and formation of new functional groups when the biomass is carbonized at different temperatures (Gopinath *et al.*, 2021). Therefore, as describe above and shown in Figure 4.5, KPJAC500 relatively contains suitable functional groups for phosphate adsorption than KPJAC400 and KPJAC600.

4.1.5. Morphological Feature Analysis

Scanning electron microscope (SEM) is one of an important and widely used method to visualize morphological properties of materials. Therefore, SEM micrographs were acquired to detect surface texture of the KPJAC400, KPJAC500, KPJAC600 and phosphate loaded KPJAC500. According to Figure 4.6a-d the KPJAC500 micrograph look like honeycomb shaped micro pores. The volatile which are removed during activation and carbonization process generate fixed carbon network with porous structure (Sayılı *et al.*, 2015). Subsequently, with increase of pyrolysis temperature the crushed into small particles of and more carbon fragment, which developed gap as honeycomb shaped porous structure.

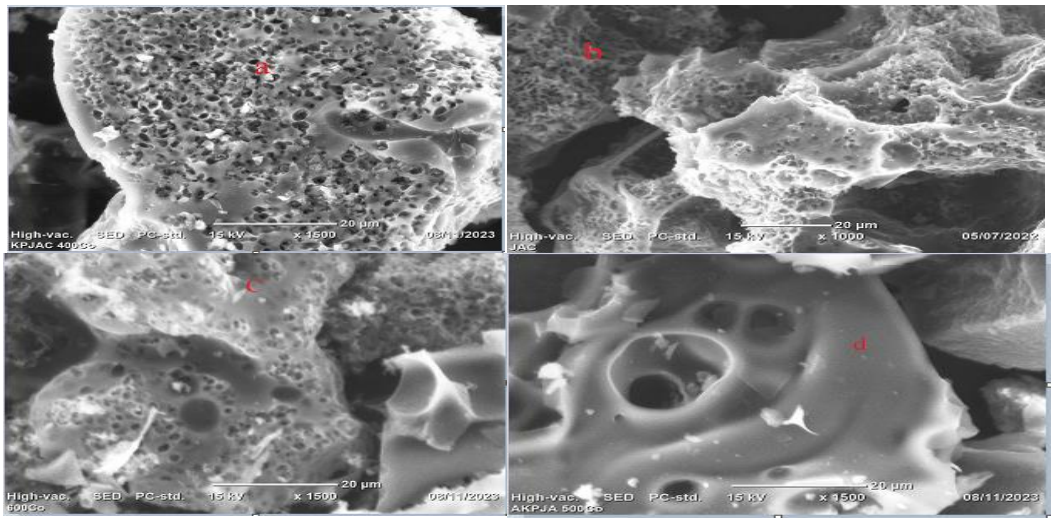

Figure 4.6: SEM micrograph for (a) KPJAC400 (b) KPJAC500 (c) KPJAC600 and (d) AKPJAC500

4.1.6. Point of Zero Charge

The solution pH condition in which the surface charge density equals to zero is termed as the pH point zero charge. It is the pH of the suspension at which the surface acidic or basic functional groups of the adsorbent no longer contribute to the pH value of the solution. The

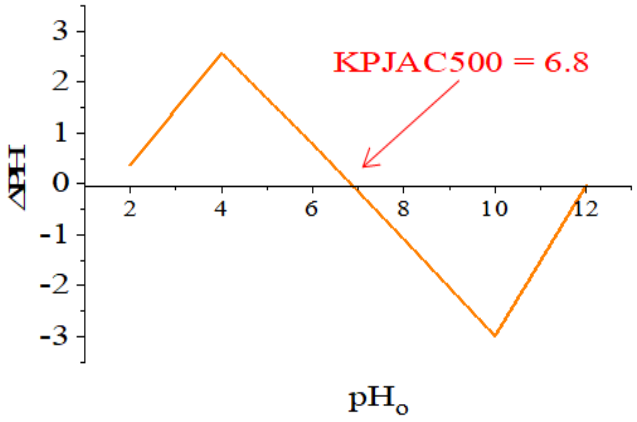

Figure 4.7: pH_{pzc} of KPJAC500

pH_{pzc} of adsorbent, potassium hydroxide treated *Prosopis Juliflora* activated carbon were evaluated from the figure of the difference between the initial and final pH values ($\Delta pH = pH_f - pH_o$) was plotted against the initial value (pH_o) as displayed in Figure 4.7, then the value of pH_{zpc} was obtained as 6.8. This result is similar to Njewa et al (2022) study report (Njewa *et al.*, 2022). From the graph, it was observed that pH< 6.8 the surface of AC is predominated by positive charge, while above pH > 6.8 the surface is dominated by negative (Stals *et al.*, 2013). Therefore, the high adsorption capacity was observed at pH< 6.8 for phosphate. For pH values of pH > 6.8 adsorption process is hindered by the repulsive electrostatic force of between adsorbent and adsorbate (Sakamoto *et al.*, 2020).

4.2. Batch Adsorption Experiment

In this study, the pretest for the adsorption capacity phosphate for PJAC, KPJAC400, KPJAC500 were measured at pH 4 using UV-visible spectrophotometer at λ = 880 nm wave length. Phosphate removal efficiency of AC prepared from *Prosopis Juliflora* wood within potassium hydroxide activating agents was shown in Table 4.2. From the table, it could be seen that the removal efficiency of HPJAC, KPJAC400, KPJAC500 and KPJAC600 were 45, 53, 81 and 77%, respectively. It could be seen that all the ACs exhibited considerable

adsorption tendency toward the phosphate. However, the KPJAC500 showed better removal of phosphate compare to other. According to Oumabady et al., (2021) research report, impregnation using potassium hydroxide involves design of the carbon frameworks by redox reaction, formation of H_2O, CO_2 and carbon gasification reaction, and finally formation of pores (microspores and mesopores) on the surface of the adsorbents (Oumabady *et al.*, 2021). In addition to microspheres structure, it occupies higher proportion of oxygenated functional groups facilitated the removal of phosphate from aqueous solution. Therefore, KPJAC500 has been selected based on FTIR, SEM and pretest of adsorption efficiency in Table 4.2.

Table 4.2: Removal efficiency of variable heat treated PJAC of PJBM adsorbent

Adsorbents	P (mg/L)	Activating agents	Adsorbent Dose (g/L)	Pyrolysis T (℃) and time (minute)	%R
HPJAC	25	Temperature	4	500 &120	45 ± 0.12
KPJAC	"	KOH	4	400 &120	58 ± 0.13
KPJAC	"	KOH	4	500 &120	83.3 ± 0.14
KPJAC	"	KOH	4	600 &120	76.7 ± 0.14

4.2.1. Optimizations for Removal of Phosphate from Aqueous Solution

4.2.1.1. Effect of pH Solution

One of the most crucial elements influencing adsorption effectiveness is pH. In this work, the following additional parameters were held constant while the impact of pH on the adsorption of phosphate from aqueous solution was assessed at various pH values between 2 and 12: 25 mg/L as the starting concentration, 4 g/L of adsorbent, and 180 minutes of contact time at

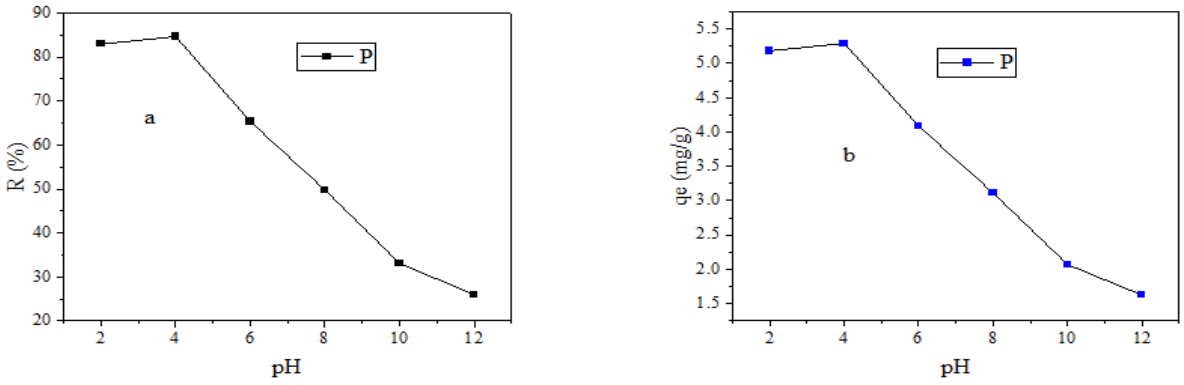

Figure 4.8: The effect of pH on (a) %R and (b) adsorption capacity for phosphate

30°C were the parameters. The results show that when the pH was raised from 2 to 4, the phosphate adsorption efficiency reached its maximum value, as shown in Figure 4.8a. The efficacy of phosphate adsorption then dramatically declined when pH rose from 4 to 12. This suggests that the ideal pH for acidic medium, where the highest phosphate absorption was seen, is reached. According to Figure 4.8b elastration, a maximum of 5.3 mg/g of phosphate absorption (qe) was observed at pH 4. This suggests that there is a greater concentration of positive charge on the surface of KPJAC500 AC, which leads to an excess of H^+ protons. By means of electrostatic contact, the phosphate ion is attached to this positive charge. The rise of hydroxide ions on the adsorbent surface may be the cause of the decrease in the percentage of phosphate ion removal in the pH range of 4 to 12; strong electrostatic forces prevent phosphate ion adsorption from occurring. Astute et al. (2019) state that the largest amount of phosphate adsorbed occurs in the pH range of 2 to 4, while the lowest amount occurs in the pH range of 4 to 10 (Astuti *et al.,* 2019b). The electrostatic repulsive force between activated carbon and the phosphate molecules resulted in a reduction in the amount of phosphate adsorbed (Bacelo *et al.*, 2020; Q Xu *et al.*, 2019).

4.2.1.2. Effect of Contact Time

The contact time is also a crucial factor for phosphate adsorption. Figure 4.9a-b shows the % R and q_e respectively of phosphate adsorption onto KPJAC500 adsorbent under variable contact time (from 30 to 420 minutes) with optimal pH and other parameters such as: dose of 4 g/L and initial concentration of phosphate 25 mg/L used per 100 mL volume of adsorbate solution at temperature 30℃. The results indicate that % R of phosphate by KPJAC500 adsorbent increased from 40 to 85% with increase in contact time from 30 to 180 minutes. After the equilibrium contact time 180 minutes, the percentage of removal of phosphate was insignificant. This phenomenal may be due to a large number of vacant active sites on the surface of adsorbent were available for phosphate adsorption during the initial stage, and after a lapse of time, the remaining vacant surface sites were difficult to be occupied due to repulsive forces between the solute molecules on the solid and bulk phases (Ngueabouo *et al.,* 2022). Therefore, 180 minutes contact time is obtained to be the optimal time in which the maximum uptake of phosphate found. The maximum q_e at optimal contact time is 5.3 mg/g according to figure 4.9b shows.

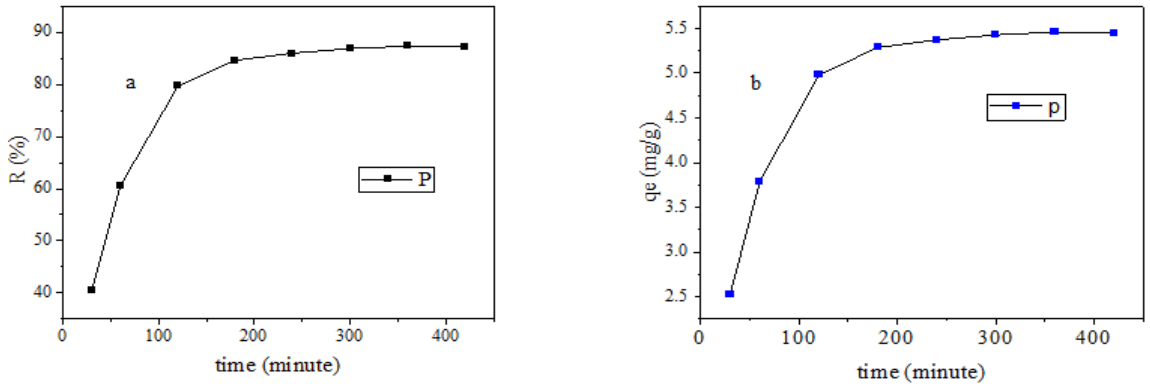

Figure 4.9: Effect of contact time KPJAC500 on (a) %R and (b) adsorption capacity (qe)

4.2.1.3. Effect of Adsorbent Dose

Assessing the adsorbent's ability to remove adsorbate requires careful consideration of dose optimization. The KPJAC500 adsorbent dosage was adjusted at various dosages (1, 2, 3, 4, 5, 6, 7, and 8 g/L) while maintaining optimal pH and contact time, a 25 mg/L adsorbate concentration, and a temperature of 30 °C per 100 mL volume of phosphate aqueous solution. This was done to ascertain the impact of the adsorbent dosage on the removal efficiency of phosphate. As shown in Figure 4. 10, the findings show that the % R of

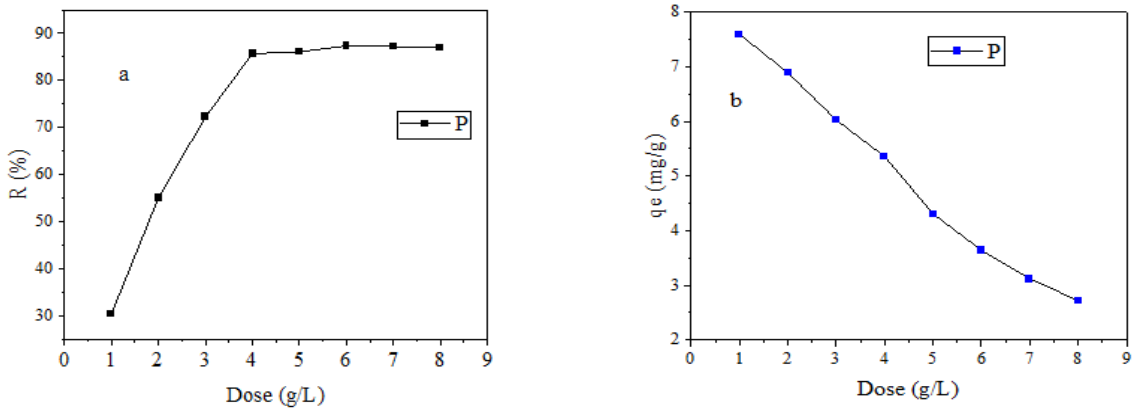

Figure 4.10: Effect of KPJAC500 adsorbent dose onto (a) %R and qe on phosphate adsorption

phosphate by KPJAC500 adsorbent rose from 45% to 85.7% with an increase in adsorbent dosage from 1 to 4 g/L. This is because more active sites will be accessible to adsorb the phosphate from the aqueous solution when the adsorbent's surface area grows with an increase in adsorbent dosage. The surface area of the adsorbent will rise as the adsorbent

dose increases in the system. This is because there are more active sites available to adsorb the phosphate ions from the aqueous solution and reach an equilibrium value. Because of adsorbent buildup and the potentially repulsion-inducing compressibility of functional groups on the adsorbent surface, the equilibrium absorption of phosphate did not appreciably increase at large adsorbent doses. Additionally, the amount of adsorbate adsorbed per unit weight of adsorbent decreases when adsorbent mass increases during adsorption (Vasudevan & Rangaiah, 2011). As a result, the KPJAC500 dose of 4 g/L is the ideal one for achieving the highest phosphate absorption. Similar result was reported by Yao et al (2018) in adsorption phosphate by AC Yao *et al.*, 2018) (Yao *et al.*, 2018).

4.2.1.4. Effect of Initial Concentration of Phosphate

The removal efficiency and absorption capacity of phosphate adsorption on the KPJAC500 adsorbent at various starting concentrations of 5, 10, 15, 20, 25, 30, and 40 mg/L are displayed in Figure 4.11a-b, respectively. Per 100 mL of phosphate solution, all other parameters remained unchanged. The outcome demonstrates that while the adsorption capacity increased from 1.12 to 5.06 mg/g with the increasing initial concentration from 5 to 25 mg/L and remained constant with the increasing initial concentration from 25 to 40 mg/L, the percentage R phosphate by the KPJAC500 adsorbent decreased from 89.60% to 50.6%.

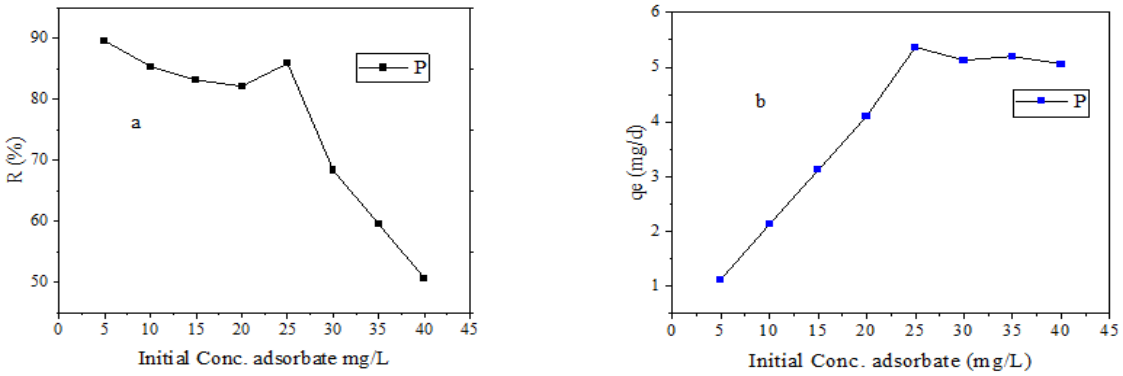

Figure 4.11: The effect of initial concentration phosphate on (a) R (%) (b) Adsorption capacity (qe) for KPJAC500

Because the chosen adsorbent lacks an active site, findings of further rising phosphate concentration indicate a reduction in % R (Mohammadi *et al.*, 2014). This shows that the highest phosphate absorption was discovered to occur at an initial phosphate concentration of

25 mg/L, which was judged to be the ideal beginning concentration. The greatest qe at the specified starting phosphate concentration is 5.37 mg/g, as shown in figure 4.11b. The elimination of phosphate diminishes dramatically when the initial concentration of phosphate in the aqueous solution rises over 30 mg/L. Because there are fewer active sites on the adsorbent at higher phosphate concentrations, the phosphate concentration between solution and the active site on the adsorbent surface as well as the mass transfer driving force are lower (Manjunath & Kumar, 2018).

4.2.1.5. Effect of temperature

To determine the thermodynamic parameter, batch adsorption studies for adsorption of phosphate onto KPJAC500 were carried out under different temperature, i.e. 293, 298, 303, 308, 313 and 318K using optimal pH, contact time, dose adsorbent and initial concentration per 100 mL volume of adsorbate solution. Then results of experiments are shown (Figure 4.12a-b), it can be observed that the % R and qe phosphate were increased from 78% to 88% and 4.9 to 5.6 mg/g respectively. The increasing % R of phosphate with increasing temperature may be due to surface activation incremental of pore on adsorbent, rising the mobility adsorbate and reduction of swelling effect of adsorbent (Manjunath *et al.*, 2017). As Table 4.3 shows that, the interpreted values of thermodynamic equilibrium constants i.e. $\Delta G°$, ΔH° and $\Delta S°$, obtained from thermodynamic plot shown in Figure 4.13. The positive $\Delta G°$ value for KPJAC500 indicates that the adsorption process is non-spontaneous in nature.

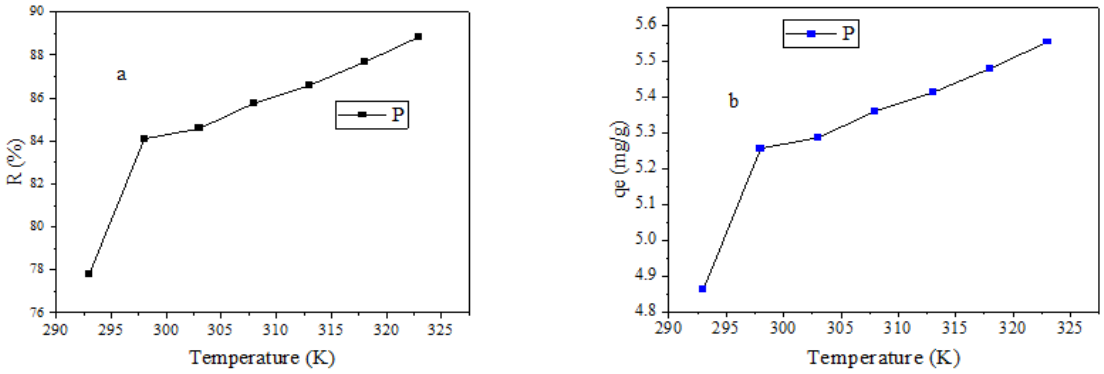

Figure 4.12: Effect of temperature (a) %R (b) absorption capacity (qe) for phosphate

However, the application of heat has resulted in the spontaneity of adsorption ($\Delta G°$ value was decreased with rising of temperature), this implies that high temperature encourage the

adsorption process (Kuete *et al.*, 2020). Additionally, the positive ΔH° demonstrates that the adsorption of phosphate on PJAC was endothermic, for which the temperature elevation accelerates the adsorption process. The rise in temperature increases the diffusion of phosphate ions in solution and in the adsorbent and increases the probability of phosphate collision with active sites (Almanassra *et al.*, 2020; X. Liu et al., 2019). An endothermic process obtain its energy form in the form of heat from surrounding molecules or environment, which could be the circumstance of chemisorption process (Tran *et al.*, 2019). Similarly, the positive ΔS° values predict increasing randomness at the solid

Table 4.3: Thermodynamic parameter for phosphate adsorption

Sample	Temperature (k)	ΔH° (KJ/mol^{-1})	ΔS° (KJ$mo^{-1}k^{-1}$)	ΔG°(KJmol^{-1})
KPJAC500	293	0.00274	0.0274	321.2828
	298			-692.17
	303			-792.373
	308			-1048.32
	313			-1246.98
	318			-1518.96

solution interface during fixation of adsorbate ions on active site of adsorbent (Lataye *et al.*, 2011). Zhang et al (2018) study report, phosphate motivated to be adsorbed on the surface of adsorbent when ΔS° values were positive (T. Zhang *et al.*, 2018). Therefore, from 323K is the optimal temperature at which the maximum uptake phosphate adsorption obtained.

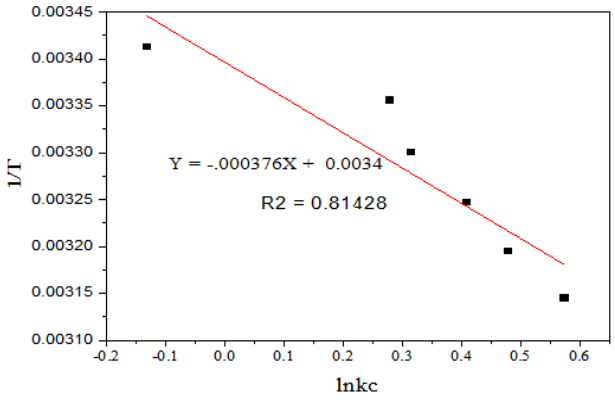

Figure 4.13: thermodynamic graph ln Kc Vs 1/t

4.2.2. Adsorption isothermal model

The adsorption isotherm indicates how the adsorbate molecules are distributed between the liquid phase and the solid phase at given pH values and temperatures. Generally, the Langmuir and Freundich isotherms were applied to study the adsorption equilibrium. The data produced from this study provides important physicochemical data for evaluating the applicability of the adsorption process. This study analyzed the equilibrium data using Langmuir and Freundlich isotherm models. These are commonly related to the type of coverage, the possibility of interaction between the adsorbent and adsorbate species, and the heterogeneity and homogeneity of the adsorbent. Isotherm models relate adsorbed adsorbate quantity over adsorbent to equilibrium adsorbate concentration at constant temperature (Rajahmundry *et al.,* 2021).

In this study, The adsorption isotherm experiments were done on different concentrations of phosphate aqueous solution (5, 10, 15, 20, 25, 30, 35 and 40 ppm) for 180 min contact time, 4 g/L of PJAC, and a volume of 100 ml solution at temperature of 30℃. The data obtained from the experiments of this study were analyzed by linear forms of Langmuir and Freundlich isotherms.

4.2.2.1. Langmuir isothermal adsorption model

The experimental data was evaluated according to the linear form of the Langmuir isotherm as described in Equation 10. The values of qm and KL are linear expression of the Langmuir

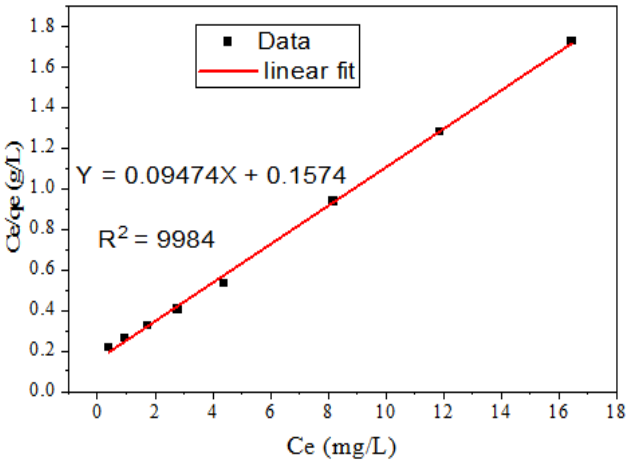

Figure 4.14: Langmuir adsorption isothermal model

adsorption isotherm were calculated from the slope and intercept of the linear plot of Ce versus Ce/qe shown in Figure 4.14. Langmuir's adsorption constant (KL) shows the degree of adsorbate-adsorbent interaction. High KL values indicate strong adsorbate-adsorbent interaction, while small KL values indicate weak adsorbate-adsorbent interaction (Prajapati *et al.*, 2016). Therefore, calculated values of isotherm parameters and the adsorption of phosphate on PJAC show high correspondence factors for the Langmuir isotherm model. The value of R^2 (0.9984) predict that the Langmuir adsorption model provide the conformity experimental data. This specify that the monolayer adsorption in phosphate's adsorption process and the presence of homogenous active sites on the adsorbent surface. Once an active site is occupied, no additional adsorption can take place at that active site (Sayılı *et al.*, 2015). These imply that the surface extents a saturation point where the maximum adsorption of the surface will be achieved. The Langmuir isotherm often applies to a homogeneous adsorption surface with the entire adsorption site having equal adsorbate affinity (Prajapati *et al.*, 2016). The value of the separation factor (R_L), called the equilibrium parameter, can be estimated by the Langmuir isotherm using Equation 11. The obtained R_L value was $0 < R_L < 1$, as shown in Table 4.4, showing that the adsorption processes of phosphate on PJAC were favorable (Desta, 2013). Therefore, phosphate adsorption, the Langmuir adsorption isotherm model good fitted the adsorption isotherm (Mangwandi *et al.*, 2014).

Table 4.4: Result summary for the line fit graph of Langmuir adsorption isotherm model

Parameter	Results
qe (mg/g)	9.90
qm(mg/g)	10.60
Intercept	0.1574
Slope	0.09474
K_L	0.5994
R_L	0.0626
R^2	0.9984

4.2.2.2. Freundlich adsorption isotherm model

The Freundich adsorption isothermal model is involved to adsorption processes that occur on heterogonous surfaces, gives an expression which specifies the surface heterogeneity and an empirical relation of active sites over heterogeneous surface and their energies (Ayawei *et al.*, 2015). The validity of the Freundlich adsorption isotherm was calculated by Equation 12, using the same set of experimental data as for the Langmuir model. To evaluate whether Freundlich adsorption isotherm model fit to the experimental value or not, the graph of log qe versus log Ce was plotted (Figure 4.16). From linear equation the Freundlich constant K_F (L/mg), and $^1/_n$ is related to the adsorption capacity of the adsorbent and the intensity of adsorption, respectively. The degree of linearity between solution concentration and adsorption is depending on n value. If the value of n >1,

Table 4.5: Results of the linear fit of Freundlich adsorption isothermal model

Parameter	Results
qe (mg/g)	14.15
Intercept	0.55499
Slope	0.42622
K_F	3.589
1/n	0.42622
R^2	0.8771

In this study, the value for 1/n of phosphate adsorption onto PJAC was less than 0.5. This is in agreement with the result obtained with (Manjunath & Kumar, 2018).

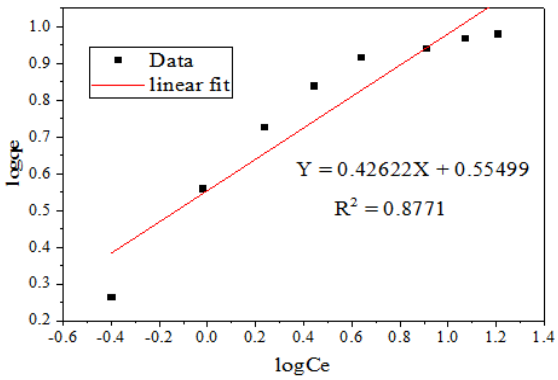

Figure 4.15: Freundlich adsorption isotherm model

then adsorption dominant by physical process may be due to distribution of active site on surface or any factors that cause decrease in adsorbent adsorbate interaction with increase surface density (Desta, 2013). In present study, the n value is greater than 1. This implies that phosphate adsorption onto PJAC was favorable. As Table 4.5 shown the value of R^2, KF and 1/n are 0.8771, 3.589 and 0.42622, respectively. The factor "1/n" in the Freundlich isotherm model can reflects the heterogeneity factor, the heterogeneity of site energies, and the adsorption intensity.

4.2.3. Adsorption kinetic model

Kinetic studies are important to select an excellent operation parameter for adsorption in batch process, which have been applicable to determine adsorption mechanisms onto adsorbent and possible rate controlling steps (Shiferaw *et al.*, 2021). To realize the uptake rate of the adsorbate, and to fix the residual time of the whole adsorption process, the pseudo-first and second-order kinetics order kinetic models were applied to fit experimental data obtained from batch experiments. The conformity between experimental data and the model-predicted values was expressed using the correlation coefficient significance (R^2). The best fitting model was selected based on correlation coefficient significance (R^2).

4.2.3.1. Pseudo-first-order kinetic model

To find out whether the adsorption process fits with the pseudo-first-order model, the experimental data was used to Equation 13. The straight-line plot of log (qe-qt) against t (Figure 4.16) gives a linear relationship from which the pseudo-first-order rate constant (K_1) and equilibrium adsorption capacity (qe) were calculated from the slope and intercept, respectively, as shown in Table 4.6. It was observed that the calculated qe values of phosphate did not agree with the experimental qe values. As Figure 4.16 shows, the pseudo-first-order kinetics model did not predict the adsorption kinetics of phosphate removal using KPJAC500, since the correlation factor R^2 was low (0.9901).

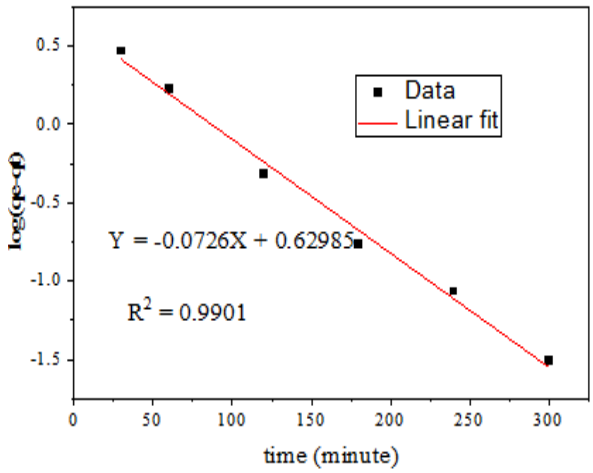

Figure 4.16: Pseudo-first order kinetic plots for adsorption of phosphate

Table 4.6: Results of the linear fit model of pseudo-first-order kinetic

Parameter	Results
Intercept	0.62985
Slope	-0.0726
qexp.(mg/g)	5.42
qe(calc.)(mg/g)	4.26
K_l	0.00726
R^2	0.9901

4.2.3.2. Pseudo-second order kinetic model

Pseudo-second order equations, a linear relationship obtain that K_2 and qe can be determined from the slop and intercept of the obtained lines. Like to the first-order kinetics model, the linearized form of the kinetic rate expression for a pseudo-second-order model was applied to the experimental data. Calculated equilibrium adsorption capacity qe (cal) and pseudo-second-order rate constant (K_2) were found from the model using Equation 14. Linear plots of t/q_t versus time are shown in Figure 4.17 for phosphate adsorbed on KPJAC500. As Figure 4.17and Table 4.7 presented the values of R^2 on pseudo-second-order for phosphate is higher than on first-order kinetics. Additional, the calculated adsorption capacity qe (cal) was closer to the experimental adsorption capacity qe (exp) than the Pseudo-first order kinetics, and since the regression coefficient, R^2 of the pseudo-second-order kinetic model is 0.9961,

which is higher than that of the pseudo-first-order kinetic model (0.9901) shows that the pseudo-second-order kinetic model designates the adsorption process of phosphate by KPJAC500

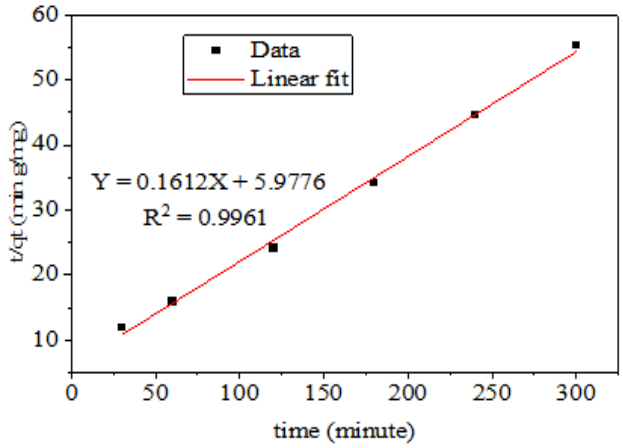

Figure 4.17: Pseudo-second order kinetic plots for adsorption of phosphate

Table 4.7: Results of the linear fit model of pseudo-second order kinetic

Parameter	Results
Intercept	5.9776
Slope	0.1612
qexp.(mg/g)	5.42
qe(calc.)(mg/g)	6.200
K_2	0.027
R^2	0.9961

4.2.4. Effect of Competitive Ions

Real wastewater contains various anionic chemicals other than phosphate ion. The coexistence of various ions in the matrix solution affects the equilibrium adsorption capacity of phosphate with activated carbon. Therefore, we studied the effect of each competitive ion on the uptake of phosphate by using 10, 25 and 50 mg/L, SO_4^{2-}, NO_3^-, Cl^- individually and the mixture by adding 4 g/L KPJAC500 in 100 mL of an aqueous solution which had an initial phosphate concentration of 25 mg/. L. As Figure 4.18 shows, that the recovery efficiency for phosphates was reduced to 36%, 27, 21% and 19% in 180 min, respectively, in the presence of interfering anions. Almanassra et al. (2020) in his study observed that

decreasing phosphate ions removal efficiency in the presence of interfering ions (Almanassra *et al.*, 2020). One possible explanation is that ionic size and the charge density of coexisting ions might account for this order (Chatterjee & De, 2017).

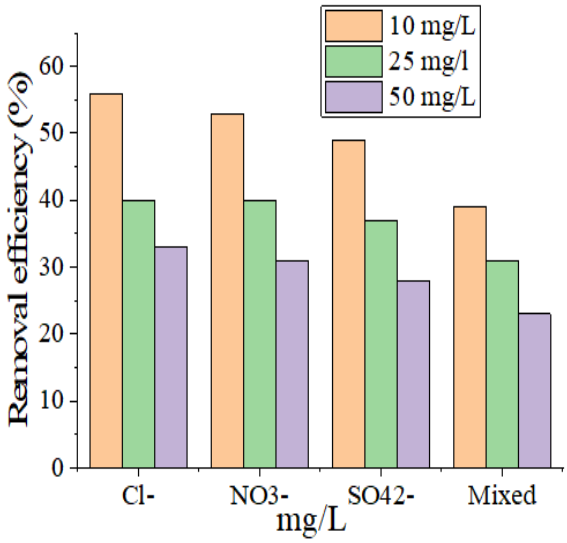

Figure 4.18: Effect of coexisting anions on the adsorption of phosphate onto KPJAC500

4.3. Adsorption of phosphate from municipal sewage onto PJAC adsorbent

Determination of the real sewerage wastewater sample physicochemical properties is important to use KPJAC500 as an adsorbent for wastewater sample. The practicability and effectiveness of an adsorption process depends not only on the properties of the adsorbent, but also on the composition of the wastewater. Real untreated wastewater sample was collected from discharging point of MSF municipal wastewater. The results of physicochemical parameter of wastewater samples analyzed in this study are showed in Table 4.8. EPA enforced a limit value of 5 mg/L of phosphate in wastewater (EPA, 2003). The municipal wastewater sample was first determined for its initial phosphate concentration by using ascorbic--molybdate method and UV-Vis spectrophotometer at λ max 880nm (Astuti *et al.*, 2019a). As shown in Table 4.8, the results presented that the phosphate concentration in the real residence wastewater sample was found above the permissible level. Therefore, the amount of phosphate found in the real wastewater sample could adversely affect aquatic environment and human health.

To evaluate the application of KPJAC500 as adsorbent for phosphate recovery from municipal wastewater, the sample was treated under optimized experimental parameters at

pH 4, contact time 180 min, adsorbent dose 0.4 g per 100 mL of volume, and at temperature 30℃ with initial concentration of phosphate 29.4 mg/L. The prepared sample obtained after treatment analyzed by UV-Vis spectrometer. The prepared PJAC adsorbent is promisingly removed phosphate from real municipal wastewater with 52.3% adsorption efficiency.

Table 4.8: Physiochemical properties of municipal wastewater sample

Parameters	Municipal Sewage	EEPA (2003) limited Standard
Temperature (℃)	33 ± 0.321	40
pH	5.8 ± 0.013	6.5-8.5
EC (µS/cm)	347 ± 0.812	1000
TDS (mg/L)	886 ± 0.851	1000
PO_4^{3-}(mg/L)	29.4 ± 0.02	5
NO_3^-(mg/g)	158 ± 0.432	20
SO_4^{2-}(mg/L)	7.2 ± 0.011	250
Cl^-(mg/L)	49 ± 0.052	250
COD (mg/L)	926 ± 0.931	250

4.4. Desorption of Adsorbate

To indicate the application sight of the material in the real situation, the elution adsorbate and reuse of adsorbent was further studied. Desorption is the most studied method to recover adsorbate and recycling adsorbents for reuse in other adsorption processes. When pH < pH_{PZC}, the surface of the KPJAC500 adsorbent was positive charged, which is encouraging to rich in equilibrium of adsorption. Therefore, the prepared adsorbent in present study had weak adsorption effect under high pH, so it fevered elution under basic circumstances. Sodium hydroxide (NaOH) solutions as the most appropriate ones for desorption due to competition of OH^- ions with adsorbed phosphate ions. The sample KPJAC500 was eluted four cycles with 0.1N NaOH solution and the adsorption efficiency was shown in Figure 4.19.

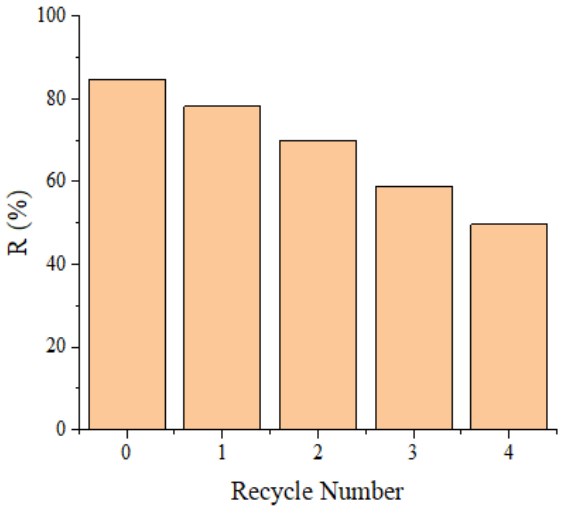

Figure 4.19: Desorption efficiency with cyclic number for phosphate adsorption

The elution experiment was conducted for four cycles. It is shown that the uptake capacity for phosphate of KPJAC decreased slightly with the elution cycle increasing, but the phosphate removal rate was decreased from 84.7 to 49.6 % after four cycles of regeneration, indicating that the adsorbent is good in regeneration and for recycling use in another adsorption. However, the adsorbent separation form aqueous solution is challenge, it biter to use as soil amendment instead reusing (Kamali *et al.,* 2020).

5. CONCLUSION AND RECOMMENDATION

5.1. Conclusion

In this work, AC adsorbent was synthesized for the removal of Phosphate from Municipal Wastewater. The as-synthesized adsorbent showed maximum removal capacity of 10.6 mg/g with removal efficiency of 84.6% at optimized pH 4, contact time of 180 minutes, initial phosphate concentration of 25 mg/L, 4g/L of dose and at temperature 30℃. The adsorption process of this study is well described by the Langmuir model with a high R^2 value of 0.9984 than Freundlich model, which indicated the adsorption mechanism is monolayer adsorption processes and the presence of homogenous sites on the prepared adsorbent surface. The data from kinetic experiments was found to fit well with the pseudo-second-order kinetic model with a high R^2 value of 0.9961, which indicates the presence of chemisorption.

5.2. Recommendation

In this work, the activated carbon was prepared from PJ, but further study is needed to produce the activated carbon from its root and seeds. To make the analysis more inclusive, preparing activated at more different activating reagent with different ratio and carbonization time is better for different inorganic (anion) adsorption.

6. REFERENCE

Abrha, B. H., & Chen, Y. (2017). Analysis of Physico-Chemical Characteristics of Effluents from Beverage Industry in Ethiopia. *Journal of Geoscience and Environment Protection*, *05*(06), 172–182. https://doi.org/10.4236/gep.2017.56016

Almanassra, I. W., Kochkodan, V., Mckay, G., Atieh, M. A., & Al-Ansari, T. (2021). Review of phosphate removal from water by carbonaceous sorbents. *Journal of Environmental Management*, *287*(November 2020), 112245. https://doi.org/10.1016/j.jenvman.2021.112245

Almanassra, I. W., Kochkodan, V., Subeh, M., Mckay, G., Atieh, M., & Al-Ansari, T. (2020). Phosphate removal from synthetic and treated sewage effluent by carbide derive carbon. *Journal of Water Process Engineering*, *36*(April), 101323. https://doi.org/10.1016/j.jwpe.2020.101323

Ambaye, T. G., Vaccari, M., van Hullebusch, E. D., Amrane, A., & Rtimi, S. (2021). Mechanisms and adsorption capacities of biochar for the removal of organic and inorganic pollutants from industrial wastewater. *International Journal of Environmental Science and Technology*, *18*(10), 3273–3294. https://doi.org/10.1007/s13762-020-03060-w

Ambroz, F., Macdonald, T. J., Martis, V., & Parkin, I. P. (2018). Evaluation of the BET theory for the characterization of meso and microporous MOFs. *Small Methods*, *2*(11), 1–17. https://doi.org/10.1002/smtd.201800173

Amin, F. R., Huang, Y., He, Y., Zhang, R., Liu, G., & Chen, C. (2016). Biochar applications and modern techniques for characterization. *Clean Technologies and Environmental Policy*, *18*(5), 1457–1473. https://doi.org/10.1007/s10098-016-1218-8

Amin, M., Shah, H. H., Iqbal, A., Farooqi, Z. U. R., Krawczuk, M., & Zia, A. (2022). Conversion of Waste Biomass into Activated Carbon and Evaluation of Environmental Consequences Using Life Cycle Assessment. *Applied Sciences (Switzerland)*, *12*(11). https://doi.org/10.3390/app12115741

APHA. (2012). *Standard Methods for the Examination of Water and Wastewater*. 1496.

Arthi, D., Gladis, E. H. E., Syamsunarno, M. B., Tambunan, I. D. G., & Ulfah, M. (2019). *Temperature carbonization effect on the quality of activated carbon based on rubber seed shell Temperature carbonization effect on the quality of activated carbon based on rubber seed shell*. https://doi.org/10.1088/1742-6596/1282/1/012043

ASTMD2866-94. "Annual Book of ASTM Standards, Standard Test Method for Bulk dansity of Activated Carbon." ASTMD2866-94, Philadelphia PA, United State of America,. , 2014. (2014). 2866.

Astuti, W., Zulaechah, L. S., & Kristian, L. (2019a). Teak Leaf-Based Activated Carbon for Phosphate Removal. *Jurnal Bahan Alam Terbarukan*, *8*(1), 52–58. https://doi.org/10.15294/jbat.v8i1.20169

Astuti, W., Zulaechah, L. S., & Kristian, L. (2019b). Teak Leaf-Based Activated Carbon for Phosphate Removal. *Jurnal Bahan Alam Terbarukan*, *8*(1), 52–58. https://doi.org/10.15294/jbat.v8i1.20169

Ayawei, N., Angaye, S. S., Wankasi, D., & Dikio, E. D. (2015). Synthesis, Characterization and Application of Mg/Al Layered Double Hydroxide for the Degradation of Congo Red in Aqueous Solution. *Open Journal of Physical Chemistry*, *05*(03), 56–70. https://doi.org/10.4236/ojpc.2015.53007

Bacelo, H., Pintor, A. M. A., Santos, S. C. R., Boaventura, R. A. R., & Botelho, C. M. S. (2020). Performance and prospects of different adsorbents for phosphorus uptake and recovery from water. *Chemical Engineering Journal*, *381*(June 2019), 122566. https://doi.org/10.1016/j.cej.2019.122566

Bagreev, A., & Bandosz, T. J. (2004). Efficient Hydrogen Sulfide Adsorbents Obtained by Pyrolysis of Sewage Sludge Derived Fertilizer Modified with Spent Mineral Oil. *Environmental Science and Technology*, *38*(1), 345–351. https://doi.org/10.1021/es0303438

Bali, M., & Gueddari, M. (2019). Removal of phosphorus from secondary effluents using infiltration–percolation process. *Applied Water Science*, *9*(3), 1–8. https://doi.org/10.1007/s13201-019-0945-5

Banik, C., Lawrinenko, M., Bakshi, S., & Laird, D. A. (2018). Impact of Pyrolysis Temperature and Feedstock on Surface Charge and Functional Group Chemistry of Biochars. *Journal of Environmental Quality*, *47*(3), 452–461. https://doi.org/10.2134/jeq2017.11.0432

Berkessa, Y. W., Mereta, S. T., & Feyisa, F. F. (2019). Simultaneous removal of nitrate and phosphate from wastewater using solid waste from factory. *Applied Water Science*, *9*(2), 1–10. https://doi.org/10.1007/s13201-019-0906-z

Bhomick, P. C., Supong, A., Karmaker, R., Baruah, M., Pongener, C., & Sinha, D. (2019). Activated carbon synthesized from biomass material using single-step KOH activation for adsorption of fluoride: Experimental and theoretical investigation. *Korean Journal of Chemical Engineering*, *36*(4), 551–562. https://doi.org/10.1007/s11814-019-0234-x

Brandi, J., & Wilson-Wilde, L. (2013). Standard methods for the examination of. In *Encyclopedia of Forensic Sciences: Second Edition* (pp. 522–527).

Breulmann, M., Schulz, E., van Afferden, M., Müller, R. A., & Fühner, C. (2018). Hydrochars derived from sewage sludge: effects of pre-treatment with water on char properties, phytotoxicity and chemical structure. *Archives of Agronomy and Soil Science*, *64*(6), 860–872. https://doi.org/10.1080/03650340.2017.1396318

Buates, J., & Imai, T. (2020). Biochar functionalization with layered double hydroxides composites: Preparation, characterization, and application for effective phosphate removal. *Journal of Water Process Engineering*, *37*(June), 101508. https://doi.org/10.1016/j.jwpe.2020.101508

Bullen, J. C., Saleesongsom, S., Gallagher, K., & Weiss, D. J. (2021). A Revised Pseudo-Second-Order Kinetic Model for Adsorption, Sensitive to Changes in Adsorbate and Adsorbent Concentrations. *Langmuir*, *37*(10), 3189–3201. https://doi.org/10.1021/acs.langmuir.1c00142

Carpenter, S. R. (1981). Submersed Vegetation: An Internal Factor in Lake Ecosystem Succession. *The American Naturalist*, *118*(3), 372–383. https://doi.org/10.1086/283829

Chandradass, J., Balasubramanian, M., Bae, D. S., Kim, J., & Kim, K. H. (2010). Effect of water to surfactant ratio (R) on the particle size of MgAl2O4 nanoparticle prepared via reverse micelle process. *Journal of Alloys and Compounds*, *491*(1–2), 28–31. https://doi.org/10.1016/j.jallcom.2009.10.213

Chatterjee, S., & De, S. (2017). Adsorptive removal of arsenic from groundwater using chemically treated iron ore slime incorporated mixed matrix hollow fiber membrane. *Separation and Purification Technology*, *179*, 357–368. https://doi.org/10.1016/j.seppur.2017.02.019

Chen, C. X., Huang, B., Li, T., & Wu, G. F. (2012). Preparation of phosphoric acid activated carbon from sugarcane bagasse by mechanochemical processing. *BioResources*, *7*(4), 5109–5116. https://doi.org/10.15376/biores.7.4.5109-5116

Chowdhary, P., Bharagava, R. N., Mishra, S., & Khan, N. (2020). Role of Industries in Water Scarcity and Its Adverse Effects on Environment and Human Health. *Environmental Concerns and Sustainable Development*, *Dm*, 235–256. https://doi.org/10.1007/978-981-13-5889-0_12

Colantoni, A., Evic, N., Lord, R., Retschitzegger, S., Proto, A. R., Gallucci, F., & Monarca, D. (2016). Characterization of biochars produced from pyrolysis of pelletized agricultural residues. *Renewable and Sustainable Energy Reviews*, *64*(2016), 187–194. https://doi.org/10.1016/j.rser.2016.06.003

Comber, S., Gardner, M., Darmovzalova, J., & Ellor, B. (2015). Determination of the forms and stability of phosphorus in wastewater effluent from a variety of treatment processes. *Journal of Environmental Chemical Engineering*, *3*(4), 2924–2930. https://doi.org/10.1016/j.jece.2015.10.002

Constantin, M., Droteea, T., & Liviu, I. (2021). *Water intake meets the Water from inside the human body – physiological , cultural , and health perspectives - Synthetic and Systematic literature review Water intake meets the Water from inside the human body – physiological , cultural , and health persp*. *September*. https://doi.org/10.12680/balneo.2021.439

Contescu, C., Adhikari, S., Gallego, N., Evans, N., & Biss, B. (2018). Activated Carbons Derived from High-Temperature Pyrolysis of Lignocellulosic Biomass. *C*, *4*(3), 51. https://doi.org/10.3390/c4030051

Dai, L., Tan, F., Li, H., Zhu, N., He, M., Zhu, Q., Hu, G., Wang, L., & Zhao, J. (2017). Calcium-rich biochar from the pyrolysis of crab shell for phosphorus removal. *Journal*

of Environmental Management, *198*, 70–74. https://doi.org/10.1016/j.jenvman.2017.04.057

Desta, M. B. (2013). Batch sorption experiments: Langmuir and freundlich isotherm studies for the adsorption of textile metal ions onto teff straw (eragrostis tef) agricultural waste. *Journal of Thermodynamics*, *1*(1). https://doi.org/10.1155/2013/375830

Devi, P., & Saroha, A. K. (2017). Utilization of sludge based adsorbents for the removal of various pollutants: A review. *Science of the Total Environment*, *578*, 16–33. https://doi.org/10.1016/j.scitotenv.2016.10.220

Dim, P. E., Mustapha, L. S., & Termtanun, M. (2021). ISOTHERMS, KINETICS AND THERMODYNAMIC STUDIES OF ADSORPTION OF Cd AND Ni FROM TEXTILE EFFLUENT WITH ACID MODIFIED CLAY. *Journal of Chemical Technology and Metallurgy*, *56*(5), 1016–1029.

Domingues, R. R., Trugilho, P. F., Silva, C. A., De Melo, I. C. N. A., Melo, L. C. A., Magriotis, Z. M., & Sánchez-Monedero, M. A. (2017). Properties of biochar derived from wood and high-nutrient biomasses with the aim of agronomic and environmental benefits. *PLoS ONE*, *12*(5), 1–19. https://doi.org/10.1371/journal.pone.0176884

Egle, L., Rechberger, H., & Zessner, M. (2015). Overview and description of technologies for recovering phosphorus from municipal wastewater. *Resources, Conservation and Recycling*, *105*, 325–346. https://doi.org/10.1016/j.resconrec.2015.09.016

Elmouwahidi, A., Bailón-García, E., Pérez-Cadenas, A. F., Maldonado-Hódar, F. J., & Carrasco-Marín, F. (2017). Activated carbons from KOH and H3PO4-activation of olive residues and its application as supercapacitor electrodes. *Electrochimica Acta*, *229*, 219–228. https://doi.org/10.1016/j.electacta.2017.01.152

Fan, G., Hong, L., Luo, J., You, Y., Zhang, J., Hua, P., Du, B., Zhan, J., Ning, R., & Bao, M. (2020). Photocatalytic inactivation of harmful algae and degradation of cyanotoxins microcystin-LR using GO-based Z-scheme nanocatalysts under visible light. *Chemical Engineering Journal*, *392*(December), 123767. https://doi.org/10.1016/j.cej.2019.123767

Fan, X., Song, J., & Peng, P. (2016). Temporal variations of the abundance and optical properties of water soluble Humic-Like Substances (HULIS) in PM2.5 at Guangzhou, China. *Atmospheric Research*, *172–173*, 8–15. https://doi.org/10.1016/j.atmosres.2015.12.024

Federal EPA. (2003). Provisional Standards for Industrial Pollution Control in Ethiopia. Prepared under the ecologically sustainable industrial development (ESID) project – US/ETH/99/068/Ehiopia, EPA/UNIDO, Addis Ababa. *Esid*, *August*, 6–108.

Fetahi, T. (2019). Eutrophication of Ethiopian water bodies: a serious threat to water quality, biodiversity and public health. *African Journal of Aquatic Science*, *44*(4), 303–312. https://doi.org/10.2989/16085914.2019.1663722

Fetene, A., Fetene, Y., & Addis, T. (2022). *Adsorptive Removal of Phosphate From Wastewater Using Ethiopian Rift Pumice : Batch Experiment Adsorptive Removal of Phosphate From Wastewater*. *13*(1). https://doi.org/10.1177/1178622120969658

Fetene, Y., & Addis, T. (2020). Adsorptive Removal of Phosphate From Wastewater Using Ethiopian Rift Pumice: Batch Experiment. *Air, Soil and Water Research*, *13*. https://doi.org/10.1177/1178622120969658

Fito, J., Said, H., Feleke, S., & Worku, A. (2019). Fluoride removal from aqueous solution onto activated carbon of Catha edulis through the adsorption treatment technology. *Environmental Systems Research*, *8*(1), 1–10. https://doi.org/10.1186/s40068-019-0153-1

Fito, J., Tefera, N., Kloos, H., & Van Hulle, S. W. H. (2019). Physicochemical Properties of the Sugar Industry and Ethanol Distillery Wastewater and Their Impact on the Environment. *Sugar Tech*, *21*(2), 265–277. https://doi.org/10.1007/s12355-018-0633-z

Foo, K. Y., & Hameed, B. H. (2012). Textural porosity, surface chemistry and adsorptive properties of durian shell derived activated carbon prepared by microwave assisted NaOH activation. *Chemical Engineering Journal*, *187*, 53–62. https://doi.org/10.1016/j.cej.2012.01.079

Fu, C. C., Tran, H. N., Chen, X. H., & Juang, R. S. (2020). Preparation of polyaminated Fe3O4@chitosan core-shell magnetic nanoparticles for efficient adsorption of phosphate in aqueous solutions. *Journal of Industrial and Engineering Chemistry*, *83*, 235–246. https://doi.org/10.1016/j.jiec.2019.11.033

Gamshadzehi, E., Nassiri, M., & Ershadifar, H. (2019). One-pot synthesis of microporous Fe 2 O 3 /g-C 3 N 4 and its application for efficient removal of phosphate from sewage and polluted seawater. *Colloids and Surfaces A: Physicochemical and Engineering Aspects*, *567*, 7–15. https://doi.org/10.1016/j.colsurfa.2019.01.029

Genanaw, W., Kanno, G. G., Derese, D., & Aregu, M. B. (2021). Effect of Wastewater Discharge From Coffee Processing Plant on River Water Quality, Sidama Region, South Ethiopia. *Environmental Health Insights*, *15*. https://doi.org/10.1177/11786302211061047

Ghorbani, M., Seyedin, O., & Aghamohammadhassan, M. (2020). Adsorptive removal of lead (II) ion from water and wastewater media using carbon-based nanomaterials as unique sorbents: A review. *Journal of Environmental Management*, *254*(October 2019), 109814. https://doi.org/10.1016/j.jenvman.2019.109814

Giraldo, L., & Moreno-Piraján, J. C. (2018). CO2 adsorption on activated carbon prepared from mangosteen peel: Study by adsorption calorimetry. *Journal of Thermal Analysis and Calorimetry*, *133*(1), 337–354. https://doi.org/10.1007/s10973-017-6725-2

Gopinath, A., Divyapriya, G., Srivastava, V., Laiju, A. R., Nidheesh, P. V., & Kumar, M. S. (2021). Conversion of sewage sludge into biochar: A potential resource in water and wastewater treatment. *Environmental Research*, *194*(May 2020), 110656.

https://doi.org/10.1016/j.envres.2020.110656

Gu, W., Xie, Q., Xing, M., & Wu, D. (2017). Enhanced adsorption of phosphate onto zinc ferrite by incorporating cerium. *Chemical Engineering Research and Design*, *117*, 706–714. https://doi.org/10.1016/j.cherd.2016.11.026

Guo, G., Zhang, K., Liu, C., Xie, S., Li, X., Li, B., Shu, J., Niu, Y., Zhu, H., Ding, M., & Zhu, W. (2020). Comparative investigation on thermal decomposition of powdered and pelletized biomasses: Thermal conversion characteristics and apparent kinetics. *Bioresource Technology*, *301*. https://doi.org/10.1016/j.biortech.2020.122732

Heidari, A., Younesi, H., Rashidi, A., & Ghoreyshi, A. A. (2014). Adsorptive removal of CO2 on highly microporous activated carbons prepared from Eucalyptus camaldulensis wood: Effect of chemical activation. *Journal of the Taiwan Institute of Chemical Engineers*, *45*(2), 579–588. https://doi.org/10.1016/j.jtice.2013.06.007

Hirunpraditkoon, S., Tunthong, N., Ruangchai, A., & Nuithitikul, K. (2011). Adsorption Capacities. *International Journal of Chemical and Molecular Engineering* , *5*(6), 491–495.

Huang, W., Zhang, Y., & Li, D. (2017). Adsorptive removal of phosphate from water using mesoporous materials: A review. *Journal of Environmental Management*, *193*, 470–482. https://doi.org/10.1016/j.jenvman.2017.02.030

Hui, T. S., & Zaini, M. A. A. (2015). Potassium hydroxide activation of activated carbon: A commentary. *Carbon Letters*, *16*(4), 275–280. https://doi.org/10.5714/CL.2015.16.4.275

Huisman, J., & Hulot, F. D. (2005). Population Dynamics of Harmful Cyanobacteria. *Harmful Cyanobacteria*, 143–176. https://doi.org/10.1007/1-4020-3022-3_7

Jabit, N. A. B. (2007). The Production and Characterization of Activated Carbon Using Local Agricultural. *Carbon*, *June*.

Jack, J., Huggins, T. M., Huang, Y., Fang, Y., & Ren, Z. J. (2019). Production of magnetic biochar from waste-derived fungal biomass for phosphorus removal and recovery. *Journal of Cleaner Production*, *224*, 100–106. https://doi.org/10.1016/j.jclepro.2019.03.120

Jiang, C., Cui, S., Han, Q., Li, P., Zhang, Q., Song, J., & Li, M. (2019). Study on Application of Activated Carbon in Water Treatment. *IOP Conference Series: Earth and Environmental Science*, *237*(2), 8–13. https://doi.org/10.1088/1755-1315/237/2/022049

Jiang, C., Jia, L., He, Y., Zhang, B., Kirumba, G., & Xie, J. (2013). Adsorptive removal of phosphorus from aqueous solution using sponge iron and zeolite. *Journal of Colloid and Interface Science*, *402*, 246–252. https://doi.org/10.1016/j.jcis.2013.03.057

Jjagwe, J., Olupot, P. W., Menya, E., & Kalibbala, H. M. (2021). Synthesis and Application of Granular Activated Carbon from Biomass Waste Materials for Water Treatment: A Review. *Journal of Bioresources and Bioproducts*, *6*(4), 292–322.

https://doi.org/10.1016/j.jobab.2021.03.003

Juntakan, Maliwan, KittinThongpat, W., & Taweekun, A. (2021). Synthesis and characterization of microporous activated carbon from rubberwood by chemical activation with KOH. *Carbon Letters*, *0123456789*. https://doi.org/10.1007/s42823-020-00224-z

Kachabi, M., Mrabet, I. El, Bencheqroun, Z., Nawdali, M., & Zaitan, H. (2019). *Synthesis and adsorption properties of activated carbon from KOH-activation of Moroccan Jujube shells for the removal of COD and color from wastewater*. *8*(2), 168–178.

Kamali, M., Jahaninafard, D., Mostafaie, A., Davarazar, M., Gomes, A. P. D., Tarelho, L. A. C., Dewil, R., & Aminabhavi, T. M. (2020). Scientometric analysis and scientific trends on biochar application as soil amendment. *Chemical Engineering Journal*, *395*, 1–54. https://doi.org/10.1016/j.cej.2020.125128

Kavitha, B., Reddy, P. V. L., Kim, B., Lee, S. S., Pandey, S. K., & Kim, K. H. (2018). Benefits and limitations of biochar amendment in agricultural soils: A review. *Journal of Environmental Management*, *227*(August), 146–154. https://doi.org/10.1016/j.jenvman.2018.08.082

Kim, K., Kim, D., Kim, T., Kim, B. G., Ko, D., Lee, J., Han, Y., Jung, J. C., & Na, H. Bin. (2019). Synthesis of mesoporous lanthanum hydroxide with enhanced adsorption performance for phosphate removal. *RSC Advances*, *9*(27), 15257–15264. https://doi.org/10.1039/c9ra00895k

Kong, X., Li, S., Stromme, M., & Xu, C. (2019). Synthesis of porous organic polymers with tunable amine loadings for CO2 capture: Balanced physisorption and chemisorption. *Nanomaterials*, *9*(7). https://doi.org/10.3390/nano9071020

Köse, T. E., & Kivanç, B. (2011). Adsorption of phosphate from aqueous solutions using calcined waste eggshell. *Chemical Engineering Journal*, *178*, 34–39. https://doi.org/10.1016/j.cej.2011.09.129

Kuete, I. T., Raoul, D., Tchuifon, T., Ndifor-angwafor, G. N., Kamdem, A. T., & Anagho, S. G. (2020). *Kinetic , Isotherm and Thermodynamic Studies of the Adsorption of Thymol Blue onto Powdered Activated Carbons from Garcinia cola Nut Shells Impregnated with H 3 PO 4 and KOH : Non-Linear Regression Analysis*. 1–27. https://doi.org/10.4236/jeas.2020.101001

Kumar, P., Sudha, S., Chand, S., & Srivastava, V. C. (2010). Phosphate removal from aqueous solution using coir-pith activated carbon. *Separation Science and Technology*, *45*(10), 1463–1470. https://doi.org/10.1080/01496395.2010.485604

Kumar, S., Islam, A. R. M. T., Hasanuzzaman, M., Salam, R., Khan, R., & Islam, M. S. (2021). Preliminary assessment of heavy metals in surface water and sediment in Nakuvadra-Rakiraki River, Fiji using indexical and chemometric approaches. *Journal of Environmental Management*, *298*(March), 113517. https://doi.org/10.1016/j.jenvman.2021.113517

Kyong, W., Kyong, Y., Sung, H., & Tae, J. (2014). Journal of Industrial and Engineering Chemistry Optimization of coagulation / flocculation for phosphorus removal from activated sludge effluent discharge using an online charge analyzing system titrator (CAST). *Journal of Industrial and Engineering Chemistry*. https://doi.org/10.1016/j.jiec.2014.02.034

Labied, R., Benturki, O., Eddine Hamitouche, A. Y., & Donnot, A. (2018). Adsorption of hexavalent chromium by activated carbon obtained from a waste lignocellulosic material (Ziziphus jujuba cores): Kinetic, equilibrium, and thermodynamic study. *Adsorption Science and Technology*, *36*(3–4), 1066–1099. https://doi.org/10.1177/0263617417750739

Lalley, J., Han, C., Li, X., Dionysiou, D. D., & Nadagouda, M. N. (2016). Phosphate adsorption using modified iron oxide-based sorbents in lake water: Kinetics, equilibrium, and column tests. *Chemical Engineering Journal*, *284*, 1386–1396. https://doi.org/10.1016/j.cej.2015.08.114

Lamberti, G. A., Chaloner, D. T., & Hershey, A. E. (2010). Linkages among aquatic ecosystems. *Journal of the North American Benthological Society*, *29*(1), 245–263. https://doi.org/10.1899/08-166.1

Lataye, D. H., Mishra, I. M., & Mall, I. D. (2011). Removal of 4-Picoline from Aqueous Solution by Adsorption onto Bagasse Fly Ash and Rice Husk Ash: Equilibrium, Thermodynamic, and Desorption Study. *Journal of Environmental Engineering*, *137*(11), 1048–1057. https://doi.org/10.1061/(asce)ee.1943-7870.0000423

Lee, J., Rai, P. K., Jeon, Y. J., Kim, K. H., & Kwon, E. E. (2017). The role of algae and cyanobacteria in the production and release of odorants in water. *Environmental Pollution*, *227*, 252–262. https://doi.org/10.1016/j.envpol.2017.04.058

Lewoyehu, M., Abeje, N., & Addisu, S. (2022). Assessment of the Pollution Load of Effluents Discharged from Higher Institutions in Ethiopia: The Case of Bahir Dar University Zenzelma Campus. *International Journal of Analytical Chemistry*, *2022*. https://doi.org/10.1155/2022/9021549

Li, H., & Pan, G. (2015). Simultaneous removal of harmful algal blooms and microcystins using microorganism- and chitosan-modified local soil. *Environmental Science and Technology*, *49*(10), 6249–6256. https://doi.org/10.1021/acs.est.5b00840

Li, R., Wang, J. J., Zhou, B., Zhang, Z., Liu, S., Lei, S., & Xiao, R. (2017). Simultaneous capture removal of phosphate, ammonium and organic substances by MgO impregnated biochar and its potential use in swine wastewater treatment. *Journal of Cleaner Production*, *147*, 96–107. https://doi.org/10.1016/j.jclepro.2017.01.069

Li, T., Lü, S., Wang, Z., Huang, M., Yan, J., & Liu, M. (2021). Lignin-based nanoparticles for recovery and separation of phosphate and reused as renewable magnetic fertilizers. In *Science of the Total Environment* (Vol. 765). Elsevier B.V. https://doi.org/10.1016/j.scitotenv.2020.142745

Liu, X., Shen, F., Smith, R. L., & Qi, X. (2019). Bioresource Technology Black liquor-derived calcium-activated biochar for recovery of phosphate from aqueous solutions. *Bioresource Technology*, *294*(38), 122198. https://doi.org/10.1016/j.biortech.2019.122198

Loganathan, P., Vigneswaran, S., Kandasamy, J., & Bolan, N. S. (2014). Removal and recovery of phosphate from water using sorption. *Critical Reviews in Environmental Science and Technology*, *44*(8), 847–907. https://doi.org/10.1080/10643389.2012.741311

Lu, H., Zhang, W., Wang, S., Zhuang, L., Yang, Y., & Qiu, R. (2013). Characterization of sewage sludge-derived biochars from different feedstocks and pyrolysis temperatures. *Journal of Analytical and Applied Pyrolysis*, *102*, 137–143. https://doi.org/10.1016/j.jaap.2013.03.004

Maki, R., & Qasim, B. (2023). *Potassium Hydroxide Activated Peanut Shell as an Effective Adsorbent for the Removal of Zinc , Lead and Cadmium from Wastewater*. *24*(1), 66–78.

Malhotra, M., Suresh, S., & Garg, A. (2018). Tea waste derived activated carbon for the adsorption of sodium diclofenac from wastewater: adsorbent characteristics, adsorption isotherms, kinetics, and thermodynamics. *Environmental Science and Pollution Research*, *25*(32), 32210–32220. https://doi.org/10.1007/s11356-018-3148-y

Malini, K., Selvakumar, D., & Kumar, N. S. (2023). Activated carbon from biomass: Preparation, factors improving basicity and surface properties for enhanced CO2capture capacity - A review. *Journal of CO2 Utilization*, *67*(November 2022), 102318. https://doi.org/10.1016/j.jcou.2022.102318

Mangwandi, C., Albadarin, A. B., Glocheux, Y., & Walker, G. M. (2014). Removal of ortho-phosphate from aqueous solution by adsorption onto dolomite. *Journal of Environmental Chemical Engineering*, *2*(2), 1123–1130. https://doi.org/10.1016/j.jece.2014.04.010

Manjunath, S. V., & Kumar, M. (2018). Evaluation of single-component and multi-component adsorption of metronidazole, phosphate and nitrate on activated carbon from Prosopıs julıflora. *Chemical Engineering Journal*, *346*, 525–534. https://doi.org/10.1016/j.cej.2018.04.013

Manjunath, S. V., Kumar, S. M., Ngo, H. H., & Guo, W. (2017). Metronidazole removal in powder-activated carbon and concrete-containing graphene adsorption systems: Estimation of kinetic, equilibrium and thermodynamic parameters and optimization of adsorption by a central composite design. *Journal of Environmental Science and Health - Part A Toxic/Hazardous Substances and Environmental Engineering*, *52*(14), 1269–1283. https://doi.org/10.1080/10934529.2017.1357406

Martínez De Yuso, A., Rubio, B., & Izquierdo, M. T. (2014). Influence of activation atmosphere used in the chemical activation of almond shell on the characteristics and adsorption performance of activated carbons. *Fuel Processing Technology*, *119*, 74–80.

https://doi.org/10.1016/j.fuproc.2013.10.024

Maruo, M., Ishimaru, M., Azumi, Y., Kawasumi, Y., Nagafuchi, O., & Obata, H. (2016). Comparison of soluble reactive phosphorus and orthophosphate concentrations in river waters. *Limnology*, *17*(1), 7–12. https://doi.org/10.1007/s10201-015-0463-6

Marya, E., Alfatah, T., & Dani, M. (2020). Synthesis and characterization of activated carbon from Bambusa vulgaris striata using two-step KOH activation. *Integrative Medicine Research*, *x x*. https://doi.org/10.1016/j.jmrt.2020.03.041

Masoumi, S., & Dalai, A. K. (2020). Optimized production and characterization of highly porous activated carbon from algal-derived hydrochar. *Journal of Cleaner Production*, *263*, 121427. https://doi.org/10.1016/j.jclepro.2020.121427

Mekonnen, D. T., Alemayehu, E., & Lennartz, B. (2020). Removal of phosphate ions from aqueous solutions by adsorption onto leftover coal. *Water (Switzerland)*, *12*(5), 1–15. https://doi.org/10.3390/W12051381

Menberu, Z., Mogesse, B., & Reddythota, D. (2021). Evaluation of water quality and eutrophication status of Hawassa Lake based on different water quality indices. *Applied Water Science*, *11*(3), 1–10. https://doi.org/10.1007/s13201-021-01385-6

Mistar, E. M., Ahmad, S., Muslim, A., Alfatah, T., & Supardan, M. D. (2018). Preparation and characterization of a high surface area of activated carbon from Bambusa vulgaris - Effect of NaOH activation and pyrolysis temperature. *IOP Conference Series: Materials Science and Engineering*, *334*(1). https://doi.org/10.1088/1757-899X/334/1/012051

Miyazato, T., Nuryono, N., Kobune, M., Rusdiarso, B., & Otomo, R. (2020). Journal of Water Process Engineering Phosphate recovery from an aqueous solution through adsorption- desorption cycle over thermally treated activated carbon. *Journal of Water Process Engineering*, *36*(April), 101302. https://doi.org/10.1016/j.jwpe.2020.101302

Moges, M. A., Schmitter, P., Tilahun, S. A., Ayana, E. K., Ketema, A. A., Nigussie, T. E., & Steenhuis, T. S. (2017). Water Quality Assessment by Measuring and Using Landsat 7 ETM+ Images for the Current and Previous Trend Perspective: Lake Tana Ethiopia. *Journal of Water Resource and Protection*, *09*(12), 1564–1585. https://doi.org/10.4236/jwarp.2017.912099

Mohammadi, S. Z., Hamidian, H., & Moeinadini, Z. (2014). High surface area-activated carbon from Glycyrrhiza glabra residue by ZnCl2 activation for removal of Pb(II) and Ni(II) from water samples. *Journal of Industrial and Engineering Chemistry*, *20*(6), 4112–4118. https://doi.org/10.1016/j.jiec.2014.01.009

Mohan, D., Sarswat, A., Ok, Y. S., & Pittman, C. U. (2014). Organic and inorganic contaminants removal from water with biochar, a renewable, low cost and sustainable adsorbent - A critical review. *Bioresource Technology*, *160*, 191–202. https://doi.org/10.1016/j.biortech.2014.01.120

Moi, F. Y., Ghazi, R. M., Zazmiezi, M., Alias, M., Aksyutin, O. E., & Lining, M. N. B.

(2018). *Corn cob based activated carbon preparation using microwave assisted potassium hydroxide activation for sea water purification Corn cob based activated carbon preparation using microwave assisted potassium hydroxide activation for sea water purification*. https://doi.org/10.1088/1742-6596/1120/1/012017

Mojoudi, N., Soleimani, M., Mirghaffari, N., Belver, C., & Bedia, J. (2019). *Uncorrected Proof through physical and chemical activation Uncorrected Proof*. 1–12. https://doi.org/10.2166/wst.2019.305

Mukome, F. N. D., Zhang, X., Silva, L. C. R., Six, J., & Parikh, S. J. (2013). Use of chemical and physical characteristics to investigate trends in biochar feedstocks. *Journal of Agricultural and Food Chemistry*, *61*(9), 2196–2204. https://doi.org/10.1021/jf3049142

Mulu, A., Ayenew, T., Berhe, S., & Hailu, A. M. (2013). Impact of Slaughterhouses Effluent on Water Quality of Modjo and Akaki River in Central Ethiopia. *International Journal of Science and Research*, *4*(3), 2319–7064. www.ijsr.net

Muthulakshmi Andal, N., & Thangamani, K. S. (2016). Chemical Science Review and Letters Removal of Direct Dye using Activated Carbon Prepared from Prosopis juliflora Bark: Isothermal, Thermodynamic and Kinetic Studies. *Chem Sci Rev Lett*, *5*(20).

Najmi, S., Hatamipour, M. S., Sadeh, P., Najafipour, I., & Mehranfar, F. (2020). Activated carbon produced from Glycyrrhiza glabra residue for the adsorption of nitrate and phosphate: batch and fixed-bed column studies. *SN Applied Sciences*, *2*(4). https://doi.org/10.1007/s42452-020-2585-7

Narvekar, A. A., Fernandes, J. B., Naik, S. P., & Tilve, S. G. (2021). Development of glycerol based carbon having enhanced surface area and capacitance obtained by KOH induced thermochemical activation. *Materials Chemistry and Physics*, *261*(December 2020), 124238. https://doi.org/10.1016/j.matchemphys.2021.124238

Nejad, M. H., Takdastan, A., Jaafarzadeh, N., Mogadam, M. A., & Mengelizadeh, N. (2013). Removal of orthophosphate from municipal wastewater using chemical precipitation process in ahvaz wastewater treatment plant, Iran. *Asian Journal of Chemistry*, *25*(5), 2565–2568. https://doi.org/10.14233/ajchem.2013.13462

Ngueabouo, A. M. S., Tagne, R. F. T., Tchuifon, D. R. T., Fotsop, C. G., Tamo, A. K., & Anagho, S. G. (2022). Strategy for optimizing the synthesis and characterization of activated carbons obtained by chemical activation of coffee husk. *Materials Advances*, *3*(22), 8361–8374. https://doi.org/10.1039/d2ma00591c

Njewa, J. B., Vunain, E., & Biswick, T. (2022). Synthesis and Characterization of Activated Carbons Prepared from Agro-Wastes by Chemical Activation. *Journal of Chemistry*, *2022*. https://doi.org/10.1155/2022/9975444

Nur, T., Johir, M. A. H., Loganathan, P., Nguyen, T., Vigneswaran, S., & Kandasamy, J. (2014). Phosphate removal from water using an iron oxide impregnated strong base anion exchange resin. *Journal of Industrial and Engineering Chemistry*, *20*(4), 1301–1307. https://doi.org/10.1016/j.jiec.2013.07.009

Ouakouak, A. K., & Youcef, L. (2016). Phosphates removal by activated carbon. *Sensor Letters*, *14*(6), 600–605. https://doi.org/10.1166/sl.2016.3664

Oumabady, S., Selvaraj, P. S., Kamaludeen, S. P. B., Ettiyagounder, P., Suganya, K., & R., S. P. (2021). Application of sludge-derived KOH-activated hydrochar in the adsorptive removal of orthophosphate. *RSC Advances*, *11*(12), 6535–6543. https://doi.org/10.1039/d0ra10943f

Pagketanang, T., Artnaseaw, A., & Wongwicha, P. (2015). Microporous Activated Carbon from KOH-Activation of Rubber Seed-Shells for Application in Capacitor Electrode. In *Energy Procedia* (Vol. 79). Elsevier B.V. https://doi.org/10.1016/j.egypro.2015.11.550

Pallarés, J., González-Cencerrado, A., & Arauzo, I. (2018). Production and characterization of activated carbon from barley straw by physical activation with carbon dioxide and steam. *Biomass and Bioenergy*, *115*(April), 64–73. https://doi.org/10.1016/j.biombioe.2018.04.015

Pariyar, P., Kumari, K., Jain, M. K., & Jadhao, P. S. (2020). Evaluation of change in biochar properties derived from different feedstock and pyrolysis temperature for environmental and agricultural application. *Science of the Total Environment*, *713*, 136433. https://doi.org/10.1016/j.scitotenv.2019.136433

Patil, B. S., & Kulkarni, K. S. (2012). Development of High Surface Area Activated Carbon From Waste Material. *International Journal of Advanced Engineering Research and Studies*, *I*(II), 2249–8974.

Prajapati, S. S., Najar, P. A. M., & Tangde, V. M. (2016). Removal of Phosphate Using Red Mud: An Environmentally Hazardous Waste By-Product of Alumina Industry. *Advances in Physical Chemistry*, *2016*. https://doi.org/10.1155/2016/9075206

Ragadhita, R., Bayu, A., & Nandiyanto, D. (2021). Indonesian Journal of Science & Technology How to Calculate Adsorption Isotherms of Particles Using Two-Parameter Monolayer Adsorption Models and Equations. *Indonesian Journal of Science & Technology*, *6*(1), 205–234.

Rajahmundry, G. K., Garlapati, C., Kumar, P. S., Alwi, R. S., & Vo, D. V. N. (2021). Statistical analysis of adsorption isotherm models and its appropriate selection. *Chemosphere*, *276*, 130176. https://doi.org/10.1016/j.chemosphere.2021.130176

Rallapalli, P. B. S., & Ha, J. H. (2020). Adsorptive removal of phosphate ions from aqueous solutions using zirconium fumarate. *Applied Chemistry for Engineering*, *31*(5), 495–501. https://doi.org/10.14478/ace.2020.1058

Ramanan, R., Kim, B. H., Cho, D. H., Oh, H. M., & Kim, H. S. (2016). Algae-bacteria interactions: Evolution, ecology and emerging applications. *Biotechnology Advances*, *34*(1), 14–29. https://doi.org/10.1016/j.biotechadv.2015.12.003

Ramli, R., Mansor, N. A. W., Purba, H. F., & Romauli, N. D. M. (2021). *Activated Carbon Producing from Young Coconut Coir and Shells to Meet Activated Carbon Needs in*

Water Purification Process Activated Carbon Producing from Young Coconut Coir and Shells to Meet Activated Carbon Needs in Water Purification Process. https://doi.org/10.1088/1742-6596/2117/1/012040

Randall, D. G., & Naidoo, V. (2018). Urine: The liquid gold of wastewater. *Journal of Environmental Chemical Engineering*, *6*(2), 2627–2635. https://doi.org/10.1016/j.jece.2018.04.012

Recepoglu, Y. K., Goren, A. Y., Orooji, Y., & Khataee, A. (2022). Carbonaceous materials for removal and recovery of phosphate species: Limitations, successes and future improvement. *Chemosphere*, *287*(P2), 132177. https://doi.org/10.1016/j.chemosphere.2021.132177

Rehman, H. A., & Razzaq, R. (2017). Benefits of Biochar on the Agriculture and Environment - A Review. *Journal of Environmental Analytical Chemistry*, *04*(03), 3–5. https://doi.org/10.4172/2380-2391.1000207

Reyhanitabar, A., Farhadi, E., Ramezanzadeh, H., & Oustan, S. (2020). Effect of pyrolysis temperature and feedstock sources on physicochemical characteristics of biochar. *Journal of Agricultural Science and Technology*, *22*(2), 547–561.

Reza, M. S., Yun, C. S., Afroze, S., Radenahmad, N., Bakar, M. S. A., Saidur, R., Taweekun, J., & Azad, A. K. (2020). Preparation of activated carbon from biomass and its' applications in water and gas purification, a review. *Arab Journal of Basic and Applied Sciences*, *27*(1), 208–238. https://doi.org/10.1080/25765299.2020.1766799

Ritt, C. L., Chisholm, B. J., & Bezbaruah, A. N. (2019). Assessment of molecularly imprinted polymers as phosphate sorbents. *Chemosphere*, *226*, 395–404. https://doi.org/10.1016/j.chemosphere.2019.03.087

Sahoo, J. K., Paikra, S. K., Mishra, M., & Sahoo, H. (2019). Amine functionalized magnetic iron oxide nanoparticles: Synthesis, antibacterial activity and rapid removal of Congo red dye. *Journal of Molecular Liquids*, *282*, 428–440. https://doi.org/10.1016/j.molliq.2019.03.033

Sahu, J. N., Acharya, J., & Meikap, B. C. (2010). Optimization of production conditions for activated carbons from Tamarind wood by zinc chloride using response surface methodology. *Bioresource Technology*, *101*(6), 1974–1982. https://doi.org/10.1016/j.biortech.2009.10.031

Saka, C., Şahin, Ö., & Küçük, M. M. (2012). Applications on agricultural and forest waste adsorbents for the removal of lead (II) from contaminated waters. *International Journal of Environmental Science and Technology*, *9*(2), 379–394. https://doi.org/10.1007/s13762-012-0041-y

Sakamoto, T., Amano, Y., & Machida, M. (2020). Phosphate ion adsorption properties of PAN-based activated carbon fibers prepared with K2CO3 activation. *SN Applied Sciences*, *2*(4). https://doi.org/10.1007/s42452-020-2465-1

Sato, T. (2013). Beyond water-intensive agriculture: Expansion of Prosopis juliflora and its growing economic use in Tamil Nadu, India. *Land Use Policy*, *35*, 283–292. https://doi.org/10.1016/j.landusepol.2013.06.001

Sayılı, H., Güzel, F., & Önal, Y. (2015). Conversion of grape industrial processing waste to activated carbon sorbent and its performance in cationic and anionic dyes adsorption. *Journal of Cleaner Production*, *93*, 84–93. https://doi.org/10.1016/j.jclepro.2015.01.009

Shiferaw, H., Alamirew, T., Dzikiti, S., Bewket, W., Zeleke, G., & Schaffner, U. (2021). Water use of Prosopis juliflora and its impacts on catchment water budget and rural livelihoods in Afar Region, Ethiopia. *Scientific Reports*, *11*(1). https://doi.org/10.1038/s41598-021-81776-6

Singh, S., Kumar, V., Datta, S., Dhanjal, D. S., Sharma, K., Samuel, J., & Singh, J. (2020). Current advancement and future prospect of biosorbents for bioremediation. *Science of the Total Environment*, *709*, 135895. https://doi.org/10.1016/j.scitotenv.2019.135895

Siyal, A. A., Shamsuddin, M. R., Low, A., & Rabat, N. E. (2020). A review on recent developments in the adsorption of surfactants from wastewater. *Journal of Environmental Management*, *254*(May 2019), 109797. https://doi.org/10.1016/j.jenvman.2019.109797

Stals, M., Vandewijngaarden, J., Wróbel-iwaniec, I., Gryglewicz, G., Carleer, R., Schreurs, S., & Yperman, J. (2013). Journal of Analytical and Applied Pyrolysis Characterization of activated carbons derived from short rotation hardwood pyrolysis char. *Journal of Analytical and Applied Pyrolysis*, *101*, 199–208. https://doi.org/10.1016/j.jaap.2013.01.009

Sukmana, H., Bellahsen, N., Pantoja, F., & Hodur, C. (2021). Adsorption and coagulation in wastewater treatment - Review. *Progress in Agricultural Engineering Sciences*, *17*(1), 49–68. https://doi.org/10.1556/446.2021.00029

Sulyman, M., Namiesnik, J., & Gierak, A. (2017). Low-cost adsorbents derived from agricultural by-products/wastes for enhancing contaminant uptakes from wastewater: A review. *Polish Journal of Environmental Studies*, *26*(2), 479–510. https://doi.org/10.15244/pjoes/66769

Tang, C., Hu, D., Cao, Q., Yan, W., & Xing, B. (2017). Silver nanoparticles-loaded activated carbon fibers using chitosan as binding agent: Preparation, mechanism, and their antibacterial activity. *Applied Surface Science*, *394*, 457–465. https://doi.org/10.1016/j.apsusc.2016.10.095

Tegene, S., Ayele, N., & Belay, L. (2019). International Journal of Advanced Research in Biological Sciences Assessment of Prosopis juliflora infestation and management options at Tendaho Sugar Estate. *Int. J. Adv. Res. Biol. Sci*, *6*(3), 191–200. https://doi.org/10.22192/ijarbs

Tibebe, D., Kassa, Y., Melaku, A., & Lakew, S. (2019). PT SC. *Microchemical Journal*. https://doi.org/10.1016/j.microc.2019.04.085

Tran, H. N., Nguyen, H. C., Woo, S. H., Nguyen, T. V., Vigneswaran, S., Hosseini-Bandegharaei, A., Rinklebe, J., Kumar Sarmah, A., Ivanets, A., Dotto, G. L., Bui, T. T., Juang, R. S., & Chao, H. P. (2019). Removal of various contaminants from water by renewable lignocellulose-derived biosorbents: a comprehensive and critical review. *Critical Reviews in Environmental Science and Technology*, *49*(23), 2155–2219. https://doi.org/10.1080/10643389.2019.1607442

Tsai, W. T., Huang, P. C., & Lin, Y. Q. (2019). Reusing cow manure for the production of activated carbon using potassium hydroxide (KOH) activation process and its liquid-phase adsorption performance. *Processes*, *7*(10). https://doi.org/10.3390/pr7100737

Üner, O., & Bayrak, Y. (2018). Graphical abstract SC. *Microporous and Mesoporous Materials*. https://doi.org/10.1016/j.micromeso.2018.04.037

Vasudevan, S., & Rangaiah, G. P. (2011). Integrated framework incorporating optimization for plant-wide control of industrial processes. *Industrial and Engineering Chemistry Research*, *50*(13), 8122–8137. https://doi.org/10.1021/ie1022139

Wang, H., Gao, B., Wang, S., Fang, J., Xue, Y., & Yang, K. (2015). Removal of Pb(II), Cu(II), and Cd(II) from aqueous solutions by biochar derived from KMnO4 treated hickory wood. *Bioresource Technology*, *197*, 356–362. https://doi.org/10.1016/j.biortech.2015.08.132

Wang, S., Chandrasekhara Rao, N., Qiu, R., & Moletta, R. (2009). Performance and kinetic evaluation of anaerobic moving bed biofilm reactor for treating milk permeate from dairy industry. *Bioresource Technology*, *100*(23), 5641–5647. https://doi.org/10.1016/j.biortech.2009.06.028

Wang, S., Guo, W., Gao, F., & Yang, R. (2017). Characterization and Pb(II) removal potential of corn straw- and municipal sludge-derived biochars. *Royal Society Open Science*, *4*(9). https://doi.org/10.1098/rsos.170402

Wang, S., Kwak, J. H., Islam, M. S., Naeth, M. A., Gamal El-Din, M., & Chang, S. X. (2020). Biochar surface complexation and Ni(II), Cu(II), and Cd(II) adsorption in aqueous solutions depend on feedstock type. *Science of the Total Environment*, *712*(Ii), 136538. https://doi.org/10.1016/j.scitotenv.2020.136538

Wang, T., Meng, D., Zhu, J., & Chen, X. (2020). Effects of pelletizing conditions on the structure of rice straw-pellet pyrolysis char. *Fuel*, *264*(December 2019), 116909. https://doi.org/10.1016/j.fuel.2019.116909

Wang, X., Chang, V. W. C., Li, Z., Chen, Z., & Wang, Y. (2021). Co-pyrolysis of sewage sludge and organic fractions of municipal solid waste: Synergistic effects on biochar properties and the environmental risk of heavy metals. *Journal of Hazardous Materials*, *412*(September 2020), 125200. https://doi.org/10.1016/j.jhazmat.2021.125200

Weber, K., & Quicker, P. (2018). Properties of biochar. *Fuel*, *217*(September 2017), 240–261. https://doi.org/10.1016/j.fuel.2017.12.054

Wu, L., Wei, C., Zhang, S., Wang, Y., Kuzyakov, Y., & Ding, X. (2019). MgO-modified biochar increases phosphate retention and rice yields in saline-alkaline soil. *Journal of Cleaner Production*, *235*, 901–909. https://doi.org/10.1016/j.jclepro.2019.07.043

Xiao, X., Chen, B., Chen, Z., Zhu, L., & Schnoor, J. L. (2018). Insight into Multiple and Multilevel Structures of Biochars and Their Potential Environmental Applications: A Critical Review. *Environmental Science and Technology*, *52*(9), 5027–5047. https://doi.org/10.1021/acs.est.7b06487

Xiong, W., Tong, J., Yang, Z., Zeng, G., Zhou, Y., Wang, D., Song, P., Xu, R., Zhang, C., & Cheng, M. (2017). Adsorption of phosphate from aqueous solution using iron-zirconium modified activated carbon nanofiber: Performance and mechanism. *Journal of Colloid and Interface Science*, *493*, 17–23. https://doi.org/10.1016/j.jcis.2017.01.024

Xu, Q., Chen, Z., Wu, Z., Xu, F., Yang, D., He, Q., Li, G., & Chen, Y. (2019). Novel lanthanum doped biochars derived from lignocellulosic wastes for efficient phosphate removal and regeneration. *Bioresource Technology*, *289*, 121600. https://doi.org/10.1016/j.biortech.2019.121600

Xu, Z., Chen, J., Zhang, X., Song, Q., Wu, J., Ding, L., Zhang, C., Zhu, H., & Cui, H. (2019). Template-free preparation of nitrogen-doped activated carbon with porous architecture for high-performance supercapacitors. *Microporous and Mesoporous Materials*, *276*, 280–291. https://doi.org/10.1016/j.micromeso.2018.09.023

Yacob, A. R., Muda, N. W., & Zaki, M. A. bin M. (2017). Kesan satu langkah pengaktifan KOH terhadap karbon terubahsuai dalam tindak balas transesterifikasi dengan dimetil karbonat. *Malaysian Journal of Analytical Sciences*, *21*(4), 820–829. https://doi.org/10.17576/mjas-2017-2104-08

Yahya, M. A., Al-Qodah, Z., & Ngah, C. W. Z. (2015). Agricultural bio-waste materials as potential sustainable precursors used for activated carbon production: A review. *Renewable and Sustainable Energy Reviews*, *46*, 218–235. https://doi.org/10.1016/j.rser.2015.02.051

Yao, S., Wang, M., Liu, J., Tang, S., Chen, H., Guo, T., Yang, G., & Chen, Y. (2018). Removal of phosphate from aqueous solution by sewage sludge-based activated carbon loaded with pyrolusite. *Journal of Water Reuse and Desalination*, *8*(2), 192–201. https://doi.org/10.2166/wrd.2017.054

Yin, Q., Wang, R., & Zhao, Z. (2018). Application of Mg–Al-modified biochar for simultaneous removal of ammonium, nitrate, and phosphate from eutrophic water. *Journal of Cleaner Production*, *176*, 230–240. https://doi.org/10.1016/j.jclepro.2017.12.117

You, X., Guaya, D., Farran, A., Valderrama, C., & Cortina, J. L. (2016). Phosphate removal from aqueous solution using a hybrid impregnated polymeric sorbent containing hydrated ferric oxide (HFO). *Journal of Chemical Technology and Biotechnology*, *91*(3), 693–704. https://doi.org/10.1002/jctb.4629

Yuan, L., Qiu, Z., Yuan, L., Tariq, M., Lu, Y., Yang, J., Li, Z., & Lyu, S. (2019). Adsorption and mechanistic study for phosphate removal by magnetic Fe3O4-doped spent FCC catalysts adsorbent. *Chemosphere*, *219*, 183–190. https://doi.org/10.1016/j.chemosphere.2018.11.132

Yusufu M. I. (2012). Production and characterization of activated carbon from selected local raw materials. *African Journal of Pure and Applied Chemistry*, *6*(9), 123–131. https://doi.org/10.5897/ajpac12.022

Zhang, J. hong, Lin, Q. mei, & Zhao, X. rong. (2014). The hydrochar characters of municipal sewage sludge under different hydrothermal temperatures and durations. *Journal of Integrative Agriculture*, *13*(3), 471–482. https://doi.org/10.1016/S2095-3119(13)60702-9

Zhang, T., Xu, H., Li, H., He, X., Shi, Y., & Kruse, A. (2018). Microwave digestion-assisted HFO/biochar adsorption to recover phosphorus from swine manure. *Science of the Total Environment*, *621*, 1512–1526. https://doi.org/10.1016/j.scitotenv.2017.10.077

Zhou, L., Xu, D., Li, Y., Pan, Q., Wang, J., Xue, L., & Howard, A. (2019). Phosphorus and nitrogen adsorption capacities of biochars derived from feedstocks at different pyrolysis temperatures. *Water (Switzerland)*, *11*(8), 1–16. https://doi.org/10.3390/w11081559

Appendix

Appendix A

A. BET result for KPJAC500 adsorbent

Horiba Instruments, Inc.
SA-9600 Series Surface Area Analyzer

Analysis Report
Jun/09/2022

Customer	: Yohannes	Operator ID	: SARA
Description	: Different Experiment	Analysis Date	: Jun/09/2022
Filename	: Yohannes.sa2	Analysis Time	: 08:34:03

Condition Settings

Room Temp	: 28.0 (°C)	Atm. Pres	: 700.0 (mm)
Gas Used	: Nitrogen	Gas Conc	: 0.100, 0.000, 0.000 %

	Channel: 1	Channel: 2	Channel: 3
Sample Name	AC		
Tube Number	1	0	0
Tare Weight	10.1120 (gm)	0.0000 (gm)	0.0000 (gm)
Sample Weight	10.1580 (gm)	0.0000 (gm)	1.0000 (gm)
Degas Temp.	300 (°C)	0 (°C)	0 (°C)
Degas Time	60 (min)	0 (min)	0 (min)
Surface Area (M²/gm)	554.143	0.000	-1.#IO
Slope	133.251	-1.#IO	-1.#IO
Intercept	3.272	-1.#IO	-1.#IO
Vm	0.007	-1.#IO	-1.#IO
BET Const	41.726	-1.#IO	-1.#IO
Pearson Coef	1.000	0.000	0.000
X[1] - 0.090	15.243	1.#IO	1.#IO
X[2] - 0.045	9.218	1.#IO	1.#IO
X[3] - 0.018	5.684	1.#IO	1.#IO

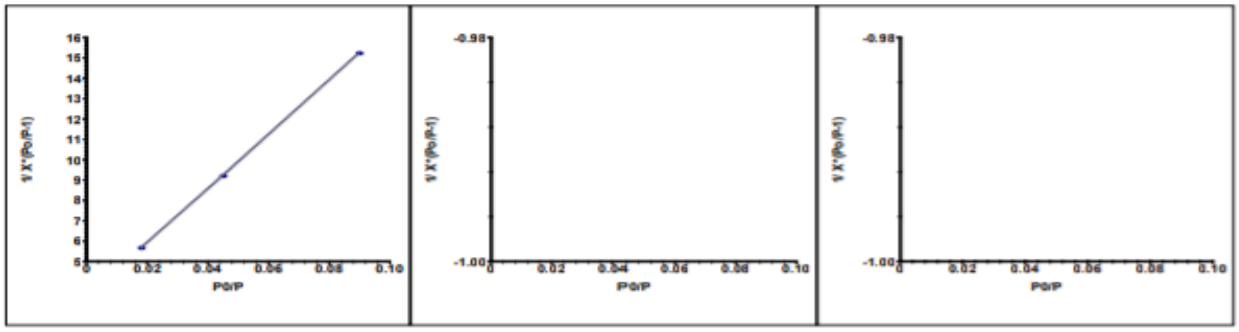

Appendix B

B. Table 6.1: Different activated carbons derived from agricultural biomass

Precursor **KOH activation**	ratio	Carbonization temp. (℃)	Paralyzing Time (minute)	S_{BET} (m2/g)	Reference
Rubber wood	1:1	600	60	287.87	(Juntakan et al., 2021)
Rubber Seed-Shells	2%	700	120	429	(Pagketanang *et al.*, 2015)
Moroccan Jujube shells	-	600	180	1067	(Mekonnen *et al.*, 2020)
Bambusa vulgaris striata	1:1	500	120	243	(Marya *et al.*, 2020)
Phyllostachys edulis	1:1	500	180	434.6	(Marya *et al.*, 2020)
Prospis Juliflora	1:1	500	120	554.143	In this study

Appendix **C**

A. C. Calculation for yield of PJAC

Fixed Carbon yield

Each 100gm of chopped *Prosopis Juliflora* raw was used for carbonization after 2 hours the carbon yield were estimated at 400, 500 and 600℃

At 400℃ of carbonization

$$\%FC\ yield = \frac{W_{PJAC}}{W_{bmPJ}} X100$$

$$W_{BM} = 100\ gm, W_{PJAC} = 55.37$$

$$\%FC\ yield = \frac{55.37\ gm}{100\ gn}\ x100$$

$$\%FC\ yield\ PJAC = 55.37$$

At 500℃ of carbonization

$$\%FC\ yield = \frac{W_{PJAC}}{W_{bmPJ}} X100$$

$$W_{BM} = 100\ gm, W_{PJAC} = 51.73\ gm$$

$$\%\text{FC yield} = \frac{51.73\ gm}{100\ gn}\ x100$$

%FC yield PJAC = 51.73

At 600℃ of carbonization

$$\%\text{FC yield} = \frac{W_{PJAC}}{W_{bmPJ}}\text{X}100$$

$$W_{BM} = 100\ gm, W_{PJAC} = 48.28\ gm$$

$$\%\text{FC yield} = \frac{48.28\ gm}{100\ gn}\ x100$$

%FC yield PJAC = 48.28

Moisture content

$$\%\text{M} = \frac{W_0 - W_d}{W_0} x100$$

At 400℃, w_0 = 1gm, w_d= 0.9453

$$\%\text{M} = \frac{1-.9453}{1}\ x100 = 5.47$$

At 500℃, w_0 = 1gm, w_d= 0.957

$$\%\text{M} = \frac{1-.957}{1}\ x100 = 4.30$$

At 600℃, w_0 = 1gm, w_d= 0.9622

$$\%\text{M} = \frac{1-.9622}{1}\ x100 = 3.78$$

Ash content

$$\%\text{Ash} = \frac{W_{ash}}{W_o}\ x100$$

At 400℃ of carbonization

$$\%\text{Ash} = \frac{0.0326gm}{1\ gm}\ x100 = 3.26$$

At 500℃ of carbonization

$$\%\text{Ash} = \frac{0.0405gm}{1\ gm}\ x100 = 4.05$$

At 600℃ of carbonization

$$\%\text{Ash} = \frac{0.0493m}{1\ gm}\ x100 = 4.93$$

Appendix D

D. Instruments used in preparation AC and adsorption process

Leaf Mill

Crushed PJAC biomass

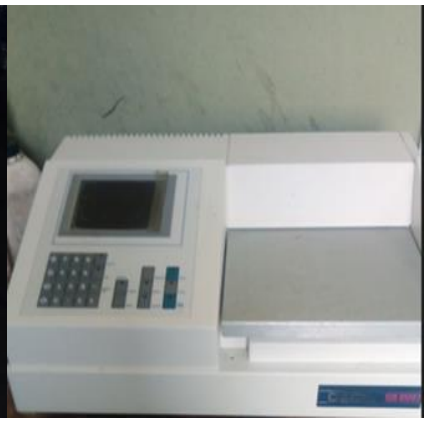

Spectrophotometer

Muffle furnace

Oven

Analytical balance

Pretest for prepared adsorbent

pH meter

Magnetic stirrer

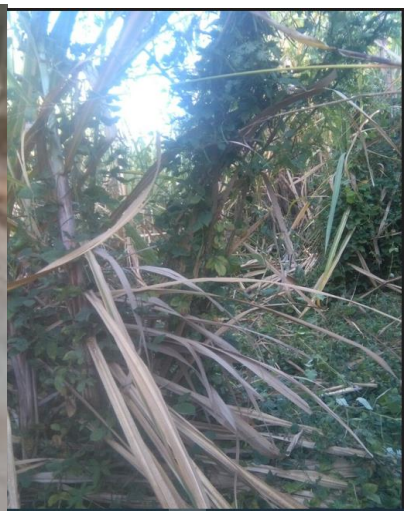

Infected Sugarcane field

Washing prepared ACs using 0.1N HCl and distilled water